
AdaRL: What, Where, and How to Adapt in Transfer Reinforcement Learning

Biwei Huang

Carnegie Mellon University
biweih@andrew.cmu.edu

Fan Feng

City University of Hong Kong
ffeng1017@gmail.com

Chaochao Lu

University of Cambridge, Max Planck Institute for Intelligent Systems
c1641@cam.ac.uk

Sara Magliacane

University of Amsterdam, MIT-IBM Watson AI Lab
sara.magliacane@gmail.com

Kun Zhang

Carnegie Mellon University
kunz1@cmu.edu

Abstract

Most approaches in reinforcement learning (RL) are data-hungry and specific to fixed environments. In this paper, we propose a principled framework for adaptive RL, called *AdaRL*, that adapts reliably to changes across domains. Specifically, we construct a generative environment model for the structural relationships among variables in the system and embed the changes in a compact way, which provides a clear and interpretable picture for locating what and where the changes are and how to adapt. Based on the environment model, we characterize a minimal set of representations, including both domain-specific factors and domain-shared state representations, that suffice for reliable and low-cost transfer. Moreover, we show that by explicitly leveraging a compact representation to encode changes, we can adapt the policy with only a few samples without further policy optimization in the target domain. We illustrate the efficacy of AdaRL through a series of experiments that allow for changes in different components of Cartpole and Atari games.

1 Introduction

Over the last years, reinforcement learning (RL) [Sutton and Barto, 1998] has seen great success in many tasks [Mnih et al., 2013, Silver et al., 2016]. However, most of these successes focus on a fixed task in a fixed environment and come at the expense of high sample complexity. Existing RL approaches are usually hard to generalize and adapt to new environments, even when the change is subtle or not directly related to decision-making. On the contrary, humans are good at transferring acquired knowledge to new environments and tasks efficiently and effectively. Generally speaking, to achieve reliable, low-cost, and interpretable transfer, it is essential to understand the underlying process—which decision-making related factors have changes, where the changes are, and how they change, instead of transferring blindly (e.g., transferring the distribution of high-dimensional images directly).

Main research lines in transfer RL include (1) adapting policies from source to the target domain and (2) finding policies that are robust to environment variations. Approaches in the first line adapt the knowledge from source domains and reuse it in the target domain, so that fewer explorations may be needed to learn the target domain policy. For example, analogous to domain adaptation, samples

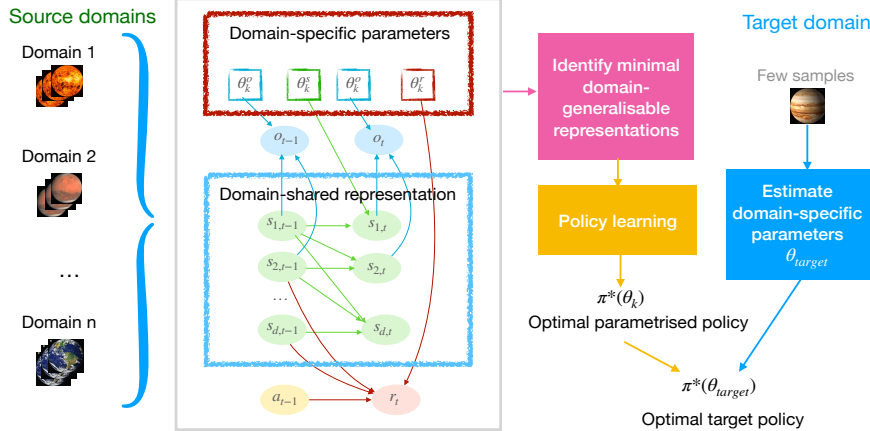


Figure 1: Diagram of the overall AdaRL framework.

$\langle s, a, r, s' \rangle$ from sources can be reused with importance reweighting [Tirinzoni et al., 2018, 2019]. Another strategy is to use the optimal source policy to initialize a learner in the target domain, as a near-optimal initializer [Taylor et al., 2007, Fernández et al., 2010]. The second line of work learns policies that are robust to environment variations, e.g., by maximizing a risk-sensitive objective over a distribution of environments [Tamar et al., 2015]. Some recent works [Zhang et al., 2020, 2021a, Tomar et al., 2021] propose methods that extract a set of invariant states for policy learning, but disregard domain-specific representations.

However, existing approaches along the first line still require a large amount of exploration and optimization in the target domain. The second line, which only leverages the invariant part, may sacrifice performance because critical information may be missed. In particular, with the increase of the number of domains, the common part could get smaller, running counter to the intention of collecting more information with more domains. Moreover, in the scenario of partially observable Markov decision processes (POMDP), most approaches do transfer on the image level, but fail to understand the changes of the underlying states, making transfer hard and unreliable [Gamrian and Goldberg, 2018].

Considering these limitations, we propose AdaRL, a transfer RL approach that achieves low-cost, reliable, and interpretable transfer for POMDPs. Specifically, it achieves quick adaptation of the optimal policy in new environments, without heavy explorations or optimizations. It also provides reliable and interpretable transfer by learning the underlying generative process and estimating factors that lead to the change across domains. Moreover, distribution shifts are usually localized – they might be due to the changes in the generative processes of only a few variables, and thus it is only necessary to adapt the distribution of a small portion of a large set of variables [Huang* et al., 2020, Schölkopf et al., 2021a], and furthermore, each module can be adapted separately [Schölkopf, 2019, Zhang* et al., 2020]. Our main contributions are summarized below and Fig. 1 gives a diagram of the overall framework of AdaRL.

- We assume a generative environment model, which explicitly takes into account the structural relationships among the system variables and embeds changes across domains in a compact way.
- Based on this model, we characterize a minimal set of representations that suffice for policy learning across domains, including the domain-specific factors of variation and state representations shared across domains. With this characterization, we adapt the policy with only a few samples without policy optimization in the target domain, achieving low-cost and reliable policy transfer.
- By leveraging a compact way to encode the changes, we also benefit from multi-task learning in model estimation. In particular, we propose the Multi-Model Structured Sequential Variational Auto-Encoder (MiSS-VAE) for reliable model estimation in general cases.

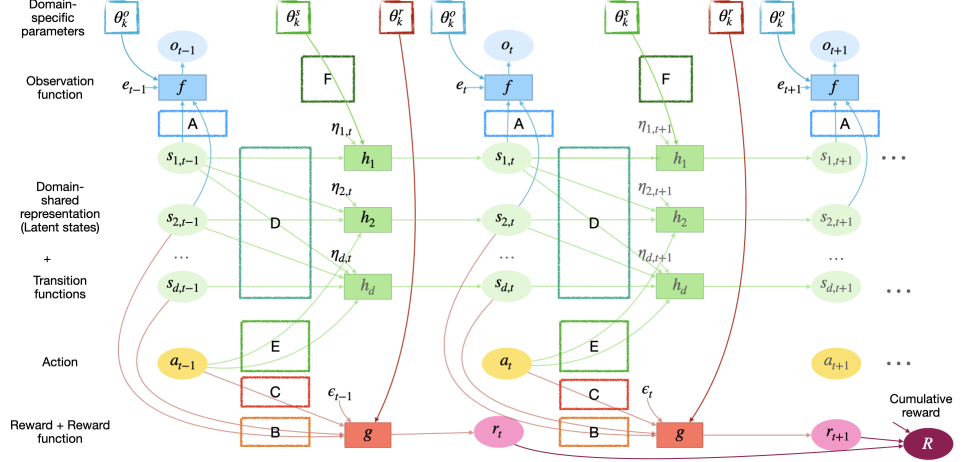


Figure 2: Graphical representation of the generative model in Eq. 1. In the top of the figure, the square boxes are the domain-specific parameters θ_k , while the filled rectangular boxes represent functions. The binary matrices A, B, C, D, E, F represent the adjacencies in this graphical representation.

2 A compact representation of environmental shifts

In this section, we formulate a generative environment model in terms of POMDPs and define a compact representation to characterize changes across domains. Suppose that there are n domains, and in each domain, we observe sequences of observations $\{\langle o_t, a_t, r_t \rangle\}_{t=1}^T$, where $o_t \in \mathcal{O}$ are the perceived signals at time t , e.g. images, $a_t \in \mathcal{A}$ is the executed action, and $r_t \in \mathcal{R}$ is the reward signal. We denote the underlying latent states by $\vec{s}_t = (s_{1,t}, \dots, s_{d,t})^\top$, where d is the dimensionality of latent states. Moreover, we allow changes in the environment model across domains. We assume that the generative process of the environment in the k -th domain can be described as:

$$\begin{aligned} o_t &= f(A \odot \vec{s}_t, \theta_k^o, e_t), \\ r_t &= g(B \odot \vec{s}_{t-1}, C \odot a_{t-1}, \theta_k^r, e_t), \\ s_{i,t} &= h_i(D_i^\top \odot \vec{s}_{t-1}, E_i^\top \odot a_{t-1}, F_i \odot \theta_k^s, \eta_{i,t}), \text{ for } i = 1, \dots, d, \end{aligned} \quad (1)$$

where \odot represents the element-wise product. The functions f , g , and h_i represent the observation function, reward function, and transition dynamics, respectively, and e_t , ϵ_t , and η_t are i.i.d. random noises. The latent states \vec{s}_t form an MDP: given \vec{s}_{t-1} and a_{t-1} , \vec{s}_t is independent of previous states and actions. The perceived signals o_t are generated from the underlying states \vec{s}_t through the observation function f perturbed by the noise e_t . The actions a_{t-1} directly influence the latent states \vec{s}_t , instead of the observed signals o_t , and the reward is determined by the latent states and the action.

We explicitly take into account the graph structure over variables in the system, similar to factored MDPs [Kearns and Koller, 1999, Boutilier et al., 2000]. This structural information is encoded in the binary matrices $A, B, C, D = [D_i]_{i=1}^d$, and $E = [E_i]_{i=1}^d$, which characterize the structural relationships among o_t, \vec{s}_t, a_t and r_t (see an illustration in Fig. 2). It allows us to model the fact that the action a_{t-1} may not influence every dimension of \vec{s}_t , the reward r_t may not be influenced by every dimension in \vec{s}_{t-1} , and also there are structural relationships between different dimensions of \vec{s}_t .

Moreover, we allow the environment to change across domains. It is commonplace that given a very high-dimensional input, only a few factors may change, which is known as *minimal change principle* [Ghassami et al., 2018] or *sparse mechanism shift assumption* [Schölkopf et al., 2021b]. In such a case, instead of learning the distribution shift over the high-dimensional input, we introduce a low-dimensional vector θ_k to characterize the domain-specific information in a compact way [Zhang* et al., 2020]. Specifically, $\theta_k = \{\theta_k^o, \theta_k^r, \theta_k^s\}$, and θ_k^o, θ_k^r , and θ_k^s capture the changing factors in the observation function, reward function, and transition dynamics, respectively; note that each of them can be multi-dimensional, and they are constant within each domain. Additionally, we use a binary matrix F to indicate the structural relationships from θ_k^s to \vec{s}_t , and F_i is its i -th row. In general, θ_k can capture the changes in the influencing strength or graph structure, e.g., some edges may vanish or appear only in some domains.

Fig. 2 gives a graphical illustration of the generative environment model in domain-varying environments, with θ_k^o , θ_k^r , and θ_k^s characterizing the changes. Specifically, in this example, θ_k^s only influences $s_{1,t}$, and also notice the graph structure over variables: a_{t-1} does not have an edge to $s_{1,t}$, and among the states, only $s_{2,t-1}$ and $s_{d,t-1}$ have edges to r_t . Note that in this example, we assume the control signals are random, so there is no edge from \vec{s}_t to a_t .

Take as an example Cartpole [Brockman et al., 2016]. The mass of the cart may vary across domains, which we can explicitly characterize by a one-dimensional factor. In this case we can directly adapt this factor alone, instead of adapting high-dimensional image sequences. On the other hand, some changes may not influence the policy, so that no adaptation is needed (e.g., in Cartpole, the change of illumination does not affect the optimal policy). With such a compact representation of changes, we can leverage multi-task learning in both model estimation and policy optimization: preserving individual information for each domain while at the same time exploiting commonalities across domains for statistically and computationally efficient optimization.

3 What, where, and how to adapt in RL

In this section, we assume that the model in Eq. (1) is known (this assumption will be relaxed in Sec. 4), and that there is no new graph edge or changing parameters in the target domain. We then answer what and where are the changes that have an effect on the policy transfer in the target domain, and how to exploit them.

In Eq. (1), we allow the model to change across domains, including all the estimated functions, and we leverage θ_k to capture the changes. The varying model implies that the optimal policy function may also vary across domains. Then we have the following question to answer: how can we characterize the changes in the optimal policy function in a compact way, as that in the model?

Interestingly, we find that a subset of θ_k is sufficient to characterize the changes in the optimal policy function. It is known that, within a domain, RL agents choose appropriate actions according to the current state vector \vec{s}_t to maximize the cumulative reward, which usually have a much lower dimensionality than that of observed images. Moreover, not every dimension of \vec{s}_t helps policy learning, in the sense that given the discounted cumulative reward $R = \sum_{t=0}^T \gamma^t r_t$, some dimensions may be conditionally independent from a_t given R and other state dimensions.

Following this intuition, we define a set of *minimal domain-generalizable representations* w.r.t. policy learning, using conditional independences to determine which dimensions of the states \vec{s}_t and of the changing factors θ_k are indispensable and sufficient for learning optimal policies across different domains.

Definition 1. Given the model in Eq. (1), we define as **minimal domain-shared representations** \vec{s}_t^{sh} w.r.t. policy learning across domains, all state dimensions $s_{i,t} \in \vec{s}_t$ satisfying

$$s_{i,t} \not\perp\!\!\!\perp a_t | R, \tilde{s}_t, \quad \forall \tilde{s}_t \subseteq \{\vec{s}_t \setminus s_{i,t}\},$$

where $\not\perp\!\!\!\perp$ is conditional dependence and R is the discounted cumulative reward. Similarly, we define as **minimal domain-specific representations** θ_k^{sp} , all the components $\theta_{i,k} \in \theta_k$ satisfying

$$\theta_{i,k} \not\perp\!\!\!\perp a_t | R, \tilde{l}_t, \quad \forall \tilde{l}_t \subseteq \{\vec{s}_t, \{\theta_k \setminus \theta_{i,k}\}\}.$$

Finally, we define as **minimal domain-generalizable representations** the union of minimal domain-shared and domain-specific representations, i.e., $\vec{s}_t^{sh} \cup \theta_k^{sp}$.

We show in the following proposition (proof in the Appendix) that *minimal domain-generalizable representations* are indeed the minimal set of dimensions that suffice for learning domain-varying policies. Such representations can be immediately identified from the graphical representation of the environment model through d-separation [Pearl, 2000], which under the causal Markov and faithfulness assumptions allows one to read all conditional dependences and independences.

Proposition 1. The minimal domain-generalizable representations contain minimal and sufficient dimensions for policy learning across domains. Moreover, given the graphical representation of the environment model, minimal domain-generalizable representations can be identified as:

- $\forall s_{i,t} \in \vec{s}_t, s_{i,t} \in \vec{s}_t^{sh}$ if and only if there is a direct or indirect edge from $s_{i,t}$ to $r_{t+\tau}$ (with $\tau \geq 1$).

- $\forall \theta_{i,k} \in \Theta_k, \theta_{i,k} \in \Theta_k^{sp}$ if and only if (1) $\theta_{i,k} \in \theta_k^r$, or (2) $\theta_{i,k} \in \theta_k^s$ and it has a direct or indirect edge to $r_{t+\tau}$ (with $\tau \geq 1$).

From the above proposition, it is easy to see that for the example illustrated in Fig. 2, $\vec{s}_t^{sh} = (s_{1,t}^\top, s_{2,t}^\top)^\top$ and $\Theta_k^{sp} = (\theta_k^{s\top}, \theta_k^{r\top})^\top$. Note that θ_k^o is not in Θ_k^{sp} , because it does not satisfy any of the conditions in Prop. 1. Thus, if only the observation function has changes, then the optimal policy function π_k^* remains the same across domains and no adaptation is needed. Also, the above analysis implies that the method proposed in [Gamrian and Goldberg, 2018] is only valid when only θ_k^o exists, where [Gamrian and Goldberg, 2018] directly transfers the image from the target domain to the source and applies the optimal source policy.

3.1 Low-cost and interpretable policy transfer

After identifying what and where to transfer, we show how to adapt. Instead of learning the optimal policy in each domain separately, which is time and sample inefficient, we leverage a multi-task learning strategy: policies in different domains are optimized at the same time exploiting both commonalities and differences across domains. Given the minimal domain-specific Θ_k^{sp} and domain-shared representations \vec{s}_t^{sh} , we represent the optimal policies across domains in a unified way:

$$a_t = \pi^*(\vec{s}_t^{sh}, \Theta_k^{sp}), \quad (2)$$

where Θ_k^{sp} explicitly and compactly encodes the changes in the policy function, and all other parameters in the optimal policy function π^* are shared across domains. In other words, if knowing π^* that is shared across domains, as well as θ_{target} and the inferred $\vec{s}_{\text{target}}^{sh}$ from the target domain, we can immediately derive the optimal policy in the target domain without further policy optimization.

We provide the pseudocode for the AdaRL algorithm in Alg. 1. The algorithm has three parts: (1) data collection with random policy or any initial policy from n source domains (line 2), (2) model estimation from the n source domains with multi-task learning (lines 2-3); see Sec. 4 for details, and (3) learning the optimal policy π^* with deep Q-learning, by making use of domain-specific factors and the inferred domain-shared state representations (lines 4-21). Specifically, because we do not directly observe the states \vec{s}_t , we infer $q(\vec{s}_{t+1,k}^{sh} | o_{\leq t+1,k}, r_{\leq t+1,k}, a_{\leq t,k}, \Theta_k^{sp})$ and sample $\vec{s}_{t+1,k}^{sh}$ from its posterior, for the k th domain (lines 7 and 13). Moreover, the action-value function Q is learned by considering the averaged error over the n source domains (line 18). AdaRL can be used with any RL algorithm, e.g. DDPG [Lillicrap et al., 2015], Q-learning [Mnih et al., 2015], and Actor-Critic methods [Schulman et al., 2015, Mnih et al., 2016].

3.2 Theoretical properties

We derive a generalization bound of AdaRL under the PAC-Bayes framework [McAllester, 1999, Shalev-Shwartz and Ben-David, 2014, Pentina and Lampert, 2014, Amit and Meir, 2018]. We assume that all domains differ in the unknown sample distribution E_k parameterized by Θ_k and that we observe the training sets $\{S_k\}_{k=1}^n$ from n different domains. For each domain, we have $S_k = ((\vec{s}_{1,k}, v^*(\vec{s}_{1,k})), \dots, (\vec{s}_{i,k}, v^*(\vec{s}_{i,k})), \dots, (\vec{s}_{m_k,k}, v^*(\vec{s}_{m_k,k})))$, where m_k is the number of samples from the k -th domain, $\vec{s}_{i,k}$ is the i -th state sampled from k -th domain, and $v^*(\vec{s}_{i,k})$ is its corresponding optimal state-value. For any value function $h_{\Theta_k^{sp}}(\cdot)$ parameterized by Θ_k^{sp} , we define the loss function $\ell(h_{\Theta_k^{sp}}, (\vec{s}_{k,i}, v^*(\vec{s}_{i,k}))) = D_{dist}(h_{\Theta_k^{sp}}(\vec{s}_{i,k}), v^*(\vec{s}_{i,k}))$.

Theorem 1. *Let \mathcal{Q} be an arbitrary distribution over Θ_k^{sp} and \mathcal{P} the prior distribution over Θ_k^{sp} . Then for any $\delta \in (0, 1]$, with probability at least $1 - \delta$, the following inequality holds uniformly for all \mathcal{Q} ,*

$$\begin{aligned} er(\mathcal{Q}) \leq & \frac{1}{n} \sum_{k=1}^n \hat{er}(\mathcal{Q}, S_k) + \frac{1}{n} \sum_{k=1}^n \sqrt{\frac{1}{2(m_k-1)} (D_{KL}(\mathcal{Q}||\mathcal{P}) + \log \frac{2nm_k}{\delta})} \\ & + \sqrt{\frac{1}{2(n-1)} (D_{KL}(\mathcal{Q}||\mathcal{P}) + \log \frac{2n}{\delta})}, \end{aligned}$$

where $er(\mathcal{Q})$ and $\hat{er}(\mathcal{Q}, S_k)$ are the generalization error and the training error between the estimated value and the optimal value, respectively.

Theorem 1 states that with high probability the generalization error $er(\mathcal{Q})$ is upper bounded by the empirical error plus a complexity term. Specifically, the first part is the average of the empirical error from observed domains, which converges to zero in the limit of samples in each domains,

Algorithm 1 (AdaRL with Domains Shifts)

```

1: Initialize action-value function  $Q$ , target action-value function  $Q'$ , and replay buffer  $\mathcal{B}$ .
2: Record multiple rollouts for each domain  $k$  ( $k = 1, \dots, n$ ) and estimate the model in Eq. (1).
3: Identify the indices of  $\bar{s}_t^{sh}$  and the values of  $\bar{s}_t^{sh}$  according to the learned model.
4: for episode = 1, ..., M do
5:   for k = 1, ..., n do
6:     Receive initial observations  $o_{1,k}$  and  $r_{1,k}$  for the  $k$ -th domain.
7:     Infer the posterior  $q(\bar{s}_{1,k}^{sh} | o_{1,k}, r_{1,k},)$  and sample  $\bar{s}_{1,k}^{sh}$ .
8:   end for
9:   for t = 1, ..., T do
10:    for k = 1, ..., n do
11:      Select  $a_{t,k}$  randomly with probability  $\epsilon$ ; otherwise select  $a_{t,k} = \arg \max_a Q(s_{t,k}^{sh}, a,)$ .
12:      Execute action  $a_{t,k}$ , and receive reward  $r_{t+1,k}$  and observation  $o_{t+1,k}$  in the  $k$ th domain.
13:      Infer the posterior  $q(\bar{s}_{t+1,k}^{sh} | o_{\leq t+1,k}, r_{\leq t+1,k}, a_{\leq t,k},)$  and sample  $\bar{s}_{t+1,k}^{sh}$ .
14:      Store transition  $(\bar{s}_{t,k}^{sh}, a_{t,k}, r_{t+1,k}, \bar{s}_{t+1,k}^{sh},)$  in reply buffer  $\mathcal{B}$ .
15:    end for
16:    Randomly sample a minibatch of  $N$  transitions  $(\bar{s}_{i,j}^{sh}, a_{i,j}, r_{i+1,j}, \bar{s}_{i+1,j}^{sh}, \theta_j^{sp})$  from  $\mathcal{B}$ .
17:    Set  $y_{i,j} = r_{i,j} + \lambda Q'(s_{i+1,j}^{sh}, \mu'(s_{i+1,j}^{sh}, \theta_j^{sp}), \theta_j^{sp})$ .
18:    Update action-value function  $Q$  by minimizing the loss:
19:      
$$L = \frac{1}{n * N} \sum_{i,j} (y_{i,j} - Q(s_{i,j}^{sh}, a_{i,j}, \theta_j^{sp}))^2.$$

20:  end for
21:  Update the target network  $Q'$ :  $Q' = Q$ .
22: end for

```

i.e., $m_k \rightarrow \infty$. The second is an environment-complexity term. It converges to zero if infinite number of domains is observed. i.e., $n \rightarrow \infty$. Moreover, if assuming different dimensions of θ_k^{sp} are independent, then $D_{KL}(Q||\mathcal{P}) = \sum_{i=1}^{|\theta_k^{sp}|} D_{KL}(Q_i||\mathcal{P}_i)$, which indicates that a low-dimensional θ_k^{sp} usually has smaller KL divergence, so does the upper bound of the generalization error.

4 Estimation of domain-varying models in one step

In this section, we give the estimation procedure of the environment model in Eq. 1 from observed sequences $\{(o_t, a_t, r_t)\}_{t=1}^T$.

Instead of estimating the model in each domain separately, we estimate models from different domains in one step, by exploiting commonalities across domains while at the same time preserving specific information for each individual domain. In particular, we develop the Multi-model Structured Sequential Variational Auto-Encoder (MiSS-VAE), which contains three essential components. (1) "Sequential VAE" component: it is used to handle the sequential data, with the underlying latent states satisfying an MDP. (2) "Multi-model" component: it handles models from different domains at the same time, with domain indices being the input. (3) "Structured" component: structural information is explicitly encoded (e.g., the latent states are organized with structures, instead of being independent as in traditional VAEs).

Let $\mathbf{y}_{t,k} = (o_{t,k}^\top, r_{t,k}^\top)^\top$, where k is the domain index, and let $\mathbf{y}_{1:T}^{1:n} = \{\{\mathbf{y}_{t,k}\}_{t=1}^T\}_{k=1}^n$. By taking into account these three components, we optimize a lower bound of the log marginal likelihood $\log P(\mathbf{y}_{1:T}^{1:n})$ with regularizers to achieve sparse graphs, minimal changes and an MDP over states:

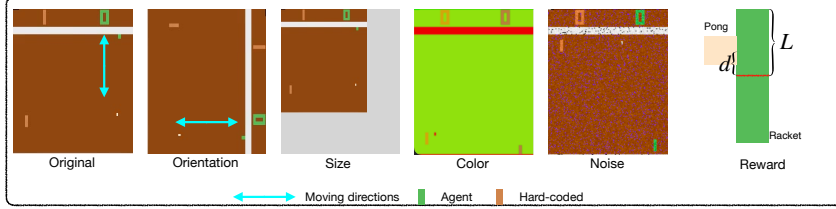


Figure 3: Illustrations of the changing factors on Pong game.

$$\begin{aligned}
& \mathcal{L}^{\text{bound}}(\mathbf{y}_{1:T}^{1:n}; (\beta, \phi, \gamma)) \\
= & \sum_{k=1}^n \sum_{t=1}^{T-2} \mathbb{E}_{q_\phi(\cdot|\theta_k)} \left\{ \underbrace{\log p_\beta(o_{t,k}|\vec{s}_{t,k}; \theta_k^o, A) + \log p_\beta(r_{t+1,k}|\vec{s}_{t,k}, a_{t,k}; \theta_k^r, B, C)}_{\text{Reconstruction}} \right. \\
& \left. + \underbrace{\log p_\beta(o_{t+1,k}|\vec{s}_{t,k}, \theta_k^o, \theta_k^s) + \log p_\beta(r_{t+2,k}|\vec{s}_{t,k}, a_{t+1,k}; \theta_k^r, \theta_k^s)}_{\text{Prediction}} \right\} \\
& - \lambda_0 \sum_{k=1}^n \sum_{t=2}^T \text{KL}(q_\phi(\vec{s}_{t,k}|\vec{s}_{t-1,k}, \mathbf{y}_{1:t,k}, a_{1:t-1,k}; \theta_k) \| \underbrace{p_\gamma(\vec{s}_{t,k}|\vec{s}_{t-1,k}, a_{t-1,k}; \theta_k^s, D, E, F)}_{\text{Transition}}) \\
& + \underbrace{\lambda_1 \|A\|_1 + \lambda_2 \|B\|_1 + \lambda_3 \|C\|_1 + \lambda_4 \|D\|_1 + \lambda_5 \|E\|_1 + \lambda_6 \|F\|_1 + \lambda_7 \sum_{1 \leq j, k \leq n} |\theta_j - \theta_k|}_{\text{Sparsity}}
\end{aligned}$$

which contains the reconstruction error, the one-step prediction error of observations, and the KL divergence to constrain the latent space. We explicitly model the transition dynamics, which is essential for establishing a Markov chain in latent space and learning a representation for long-term predictions. Furthermore, according to the edge-minimality property [Zhang and Spirtes, 2011] and the minimal change principle, we put sparsity constraints on structural matrices and on the change of domain-specific factors across domains, respectively, to achieve better identifiability. We denote by p_β the generative model with parameters β that are shared across domains, q_ϕ the inference model with shared parameters ϕ , and p_γ the transition dynamics with shared parameters γ . The structural relationships (encoded in binary matrices A, B, C, D, E , and F) are also involved in the shared parameters. Each factor is modeled with a mixture of Gaussians; with a suitable number of Gaussians, it can approximate any continuous distribution.

Moreover, in model estimation, the domain-specific factors $\theta_k = \{\theta_k^o, \theta_k^s, \theta_k^r\}$ are treated as parameters; they are constant within the same domain, but may differ in different domains. We explicitly consider θ_k not only in the generative models p_β and p_γ , but also in the inference model q_ϕ . The reason is that in this way, except θ_k , all other parameters are shared across domains, so that all we need to update in the target domain is the low-dimensional θ_k , which greatly improves the sample efficiency and the statistical efficiency in the target domain—usually few samples are needed.

5 Evaluation

We modify the Cartpole and Atari environments in OpenAI Gym [Brockman et al., 2016] with high-dimensional images as inputs, instead of the underlying states. We consider changes in the state dynamics (e.g., the change of gravity or cart mass in Cartpole, or the change of orientation in Atari), changes in perceived signals (e.g., different noise levels on observed images or different colors in Atari, as shown in Fig. A10), and changes in reward functions (e.g., different reward signals in Atari games). We train on n source domains and each domain contains 10,000 trials with 40 steps, generated by a random policy. In target domains, we consider different sample sizes with $N_{\text{target}} = 10, 50, 100, 1000, 10000$ to estimate $\theta_{\text{target}}^{\text{sp}}$. Note that we do not do policy optimization in target domains, the target data are only used for learning $\theta_{\text{target}}^{\text{sp}}$.

Modified Cartpole Setting The Cartpole problem consists of a cart and a vertical pendulum attached to the cart using a passive pivot joint. The cart can move left or right. The task is to prevent

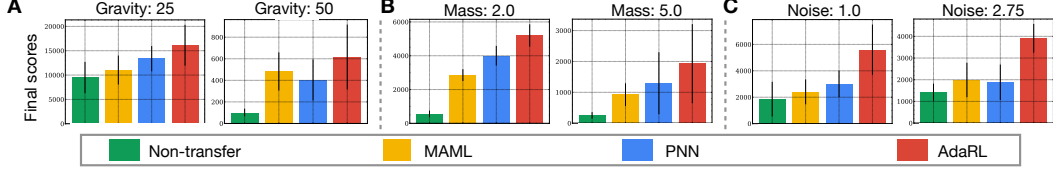


Figure 4: Average final score on Cartpole across 30 trials with changing: **A.** gravity, **B.** mass, and **C.** noise level. The left and right columns indicate the interpolation and extrapolation sets. Here, $N_{target} = 10,000$; with fewer samples the performance gain of AdaRL is even larger; see Appendix.

the vertical pendulum from falling by putting a force on the cart to move it left or right. The action space consists of two actions: moving left or right.

We introduce two changing factors for the state dynamics θ_k^s : varying gravity and varying mass of the cart. Specifically, in the gravity case, we consider source domains with gravity $g = \{5, 10, 20, 30, 40\}$. We take into account both interpolation (where the gravity in the target domain is in the support of that in source domains) with $g = \{15, 25, 35, 45\}$, and extrapolation (where it is out of the support w.r.t. the source domains) with $g = \{2, 50, 55\}$. Similarly, we consider source domains where the mass of the cart is $m = \{0.5, 1.5, 2.5, 3.5, 4.5\}$, while in target domains it is $m = \{0.2, 1.0, 2.0, 3.0, 4.0, 5.0, 5.5\}$. In terms of changes on the observation function θ_k^o , we add Gaussian noise on the images with standard deviation $\sigma = \{0.25, 0.75, 1.25, 1.75, 2.25\}$ in source domains, and $\sigma = \{0, 0.5, 1.0, 1.5, 2.0, 2.5, 2.75\}$ in target domains. Since θ_k^o does not influence the optimal policy (as shown in Prop. 1), we need it only for the model estimation, but not for policy optimization. Moreover, if $\theta_k = \{\theta_k^o\}$, the optimal policy is shared across domains.

Modified Pong setting We also evaluate AdaRL on Pong, one of the well-established Atari benchmarks. The agent controls a paddle moving up and down vertically, aiming at hitting the ball. The goal for the agent is to reach higher scores, which are earned when the other agent (hard-coded) fails to hit back the ball. We consider changes in state dynamics θ_k^s , observation function θ_k^o , and reward function θ_k^r , as illustrated by the examples in Fig. A10. Similar to Cartpole, we choose the changing factors in target domains both by interpolation and extrapolation of those in source domains. In particular, to change the state dynamics, we rotate the images to different degrees clockwise. In source domains, the degrees are chosen from $\angle = \{0^\circ, 180^\circ\}$, and in target domains, they are chosen from $\angle = \{90^\circ, 270^\circ\}$. Moreover, we consider three changing factors on perceived signals θ_k^o : different image sizes, different image colors, and different noise levels. For the image size, we reduce the original image by a factor of $\{2, 4, 6, 8\}$ in source domains and by a factor of $\{1, 3, 5, 7, 9\}$ in target domains. For the background color, we consider source domains with varying RGB colors $\{\text{original, green, red}\}$ and target domains with colors $\{\text{yellow, white}\}$. The noise-level values are the same as in the Cartpole experiments.

Finally, to test the changes in the reward function, we add two new types of reward functions: linear and non-linear reward functions. In both, the reward is a function of the distance between contact point and the central point of the paddle, as opposed to the original Pong setting in which the reward is a constant. We denote as d is the distance between contact point of the ball on the paddle and the central point of the paddle, and as L the half-length of the paddle. We use $\alpha = d/L$ to indicate the normalized distance. We then formulate the two groups of reward functions as:

1. Linear reward functions: $r_t = k_1 \alpha$
2. Non-linear reward functions: $r_t = \frac{k_2}{\alpha+3}$.

where, k_1 and k_2 are constants that we will change in the source and target domains. In group 1, we use $k_1 \in \{0.1, 0.2, 0.3, 0.4, 0.6, 0.7, 0.8\}$ in source domains and $k_1 \in \{0.5, 0.9\}$ in target domains. In group 2, we use $k_2 \in \{2.0, 3.0, 5.0, 6.0, 7.0, 8.0, 9.0\}$ in source domains and $k_1 \in \{1.0, 4.0\}$ in target domains.

Baselines We compare the convergence speed and final scores of AdaRL with a representative transfer RL method (Progressive neural networks, PNN [Rusu et al., 2016]) and a meta RL method (Model-Agnostic Meta-Learning, MAML [Finn et al., 2017]). Both of these methods have also

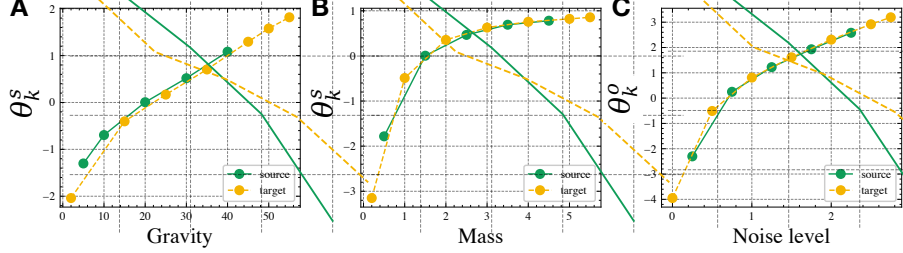


Figure 5: The estimated θ_k^{sp} for the three changing factors: gravity (A), mass (B), and noise level (C) for $N_{target} = 10,000$. Results with other sample sizes are in Appendix.

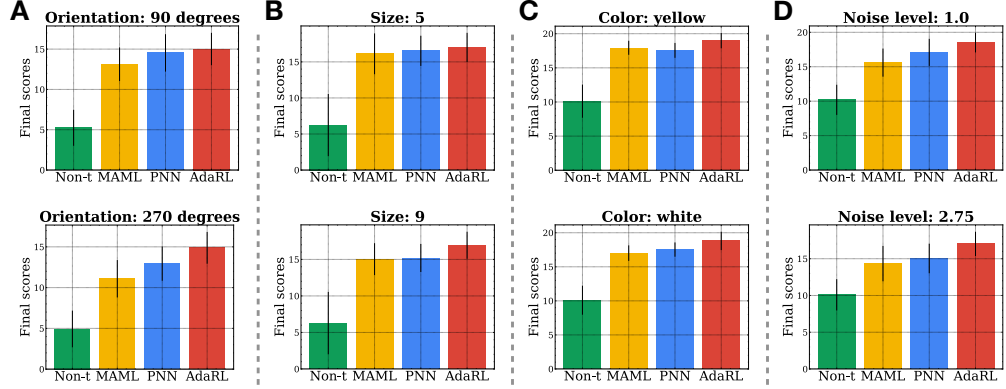


Figure 6: Average final score on Pong across 30 trials with changing: A. orientation, B. image size, C. background color, D. noise level. The top and bottom rows are the interpolation and extrapolation sets. Here, $N_{target} = 10,000$, with fewer samples the performance gain is even larger (see Fig. 8.B).

access to N_{target} samples from the target domain. We also compare with a vanilla non-transfer baseline (Non-t) that pools data from all source domains and learns a fixed model without considering the distribution shifts. For a fair comparison, we use the same policy learning algorithm, Double DQN [Van Hasselt et al., 2016], for all methods. As opposed to MAML and PNN, AdaRL only uses the N_{target} samples to estimate θ_{target}^{sp} and uses it as input to the optimal policy π^* learned across source domains, without any policy exploration.

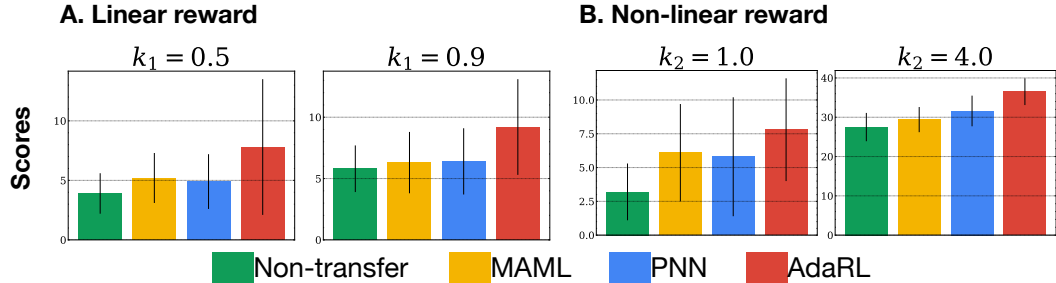


Figure 7: Average final scores on modified Pong across 30 trials with changing reward functions. Here, $N_{target} = 50,000$.

Modified Cartpole results As shown in Fig. 4, AdaRL achieves better performances than all baselines across all changing factors. We measure performance as the mean and standard deviation of the final scores over 30 trials with different random seeds. Both PNN and MAML have comparable performances, while the performance of the non-transfer baseline is much worse. Moreover, Fig. 5 shows the estimated θ_k^{sp} for the gravity, mass and noise-varying scenarios, both in source and target domains. As expected, for the gravity and noise-varying cases, we find that the learned θ_k^s and θ_k^o are

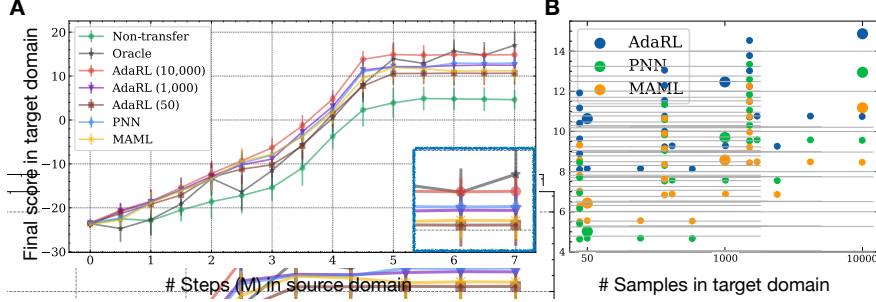


Figure 8: **A.** Average policy learning curve over 250 runs for Pong with changing orientations, in the right bottom corner there is a zoom of the scores at the final steps; **B.** Average final score over 10 runs in target domains versus different sample sizes using PNN, MAML, and AdaRL.

linear mappings of the gravity and noise level values. For the mass-varying case, the learned θ_k^s is a nonlinear monotonic function of the mass, which matches the influence of the mass on the state dynamics.

Modified Pong results In Fig. 6 we show the final score in target domains for AdaRL, MAML, PNN and the non-transfer baseline under different changes for $N_{target} = 10,000$. AdaRL consistently outperforms all other methods, with the non-transfer baseline as expected the worst, while PNN [Rusu et al., 2016] seems to provide a better performance than MAML [Finn et al., 2017] in most cases. For each factor, we give the results of 2 testing domains from both the interpolation (top) and extrapolation sets (bottom row). Interestingly, the performance gains of AdaRL with respect to the baselines are even slightly bigger in the extrapolation set, which is the more challenging setting. Fig. 7 provides the results for the final score in target domains with changing reward functions. Here, $N_{target} = 50,000$ and the results with other N_{target} are provided in Appendix. Also in this setting AdaRL outperforms other baselines. As expected, non-transfer performs the worst, while the performances of both PNN and MAML are comparable across domains.

Fig. 8A shows the evolution of the score in the target domain versus the number of steps during policy learning in the source domains. In this example, the changing factor is the orientation with a $\angle = 270^\circ$ rotation (more results are in Appendix). For PNN and MAML, we also use $N_{target} = 10,000$ samples from target domains for the adaptation. From Fig. 8, we find that even with only a few samples for model estimation(i.e., 50 samples), the performance of AdaRL is still comparable with PNN and MAML when they use 10,000 samples, while for $N_{target} = 10,000$, AdaRL improves faster than the baselines. On the other hand, the behavior of PNN and MAML on fewer samples (e.g. $N_{target} = 50$) is close to the non-transfer baseline (Fig. 8B), which shows the even larger advantage of using AdaRL when only few samples are available in the target domain.

We also plot the behaviour of an "oracle" policy that is completely trained on the target domain (in this case, the x-axis represents the steps that are used in the target domain). We show that AdaRL's performance (which only uses N_{target} samples to estimate θ_k^{sp}) is very close to the policy learning curve of the oracle. This shows that the parametrized policy is optimal in the target domain.

6 Related work

Our work lies at the interaction of transfer learning, meta-learning, and multi-task learning in the context of RL. In particular, there have been various approaches in transfer RL, differing in what knowledge is transferred [Taylor and Stone, 2009, Zhu et al., 2020]. Besides those that are mentioned in Sec. 1, *reward shaping* leverages the exterior knowledge to reconstruct the reward distributions of the target domain to guide policy learning [Ng et al., 1999]. *Learning from demonstrations* is another technique to assist RL by utilizing provided demonstrations for more efficient exploration [Hester et al., 2018]. Our work is also related to meta-learning in RL [Finn et al., 2017, Mendonca et al., 2019, Duan et al., 2016, Zintgraf et al., 2019, Nagabandi et al., 2018], which uses data from multiple tasks to learn how to learn. In practice, the performance of meta-learning algorithms depends on the user-specified meta-training task distribution [Gupta et al., 2018]. Another widely-

used technique is finetuning: a model is pretrained on a source domain and the output layers are finetuned via backpropagation in the target domain [Hinton and Salakhutdinov, 2006, Mesnil et al., 2012]. PNN, instead, retains a pool of pretrained models and learn lateral connections from them to extract useful features for the new task [Rusu et al., 2016]. Regarding multi-task learning in RL, representative methods include DISTRAL [Teh et al., 2017], IMPALA [Espeholt et al., 2018], and PopArt [Hessel et al., 2019]. The uniqueness of our proposed AdaRL, compared to state-of-the-art, is that it clearly characterizes the structural relationships and makes use of the property of graphical models, embedding changes in a compact way, to achieve low-cost and interpretable transfer.

On the other hand, since our work makes use of structural relationships, it is also related to factored MDP [Kearns and Koller, 1999, Boutilier et al., 2000, Strehl et al., 2007], Bayesian network learning, and causality [Spirtes et al., 1993, Pearl, 2000]. Some recent works [Zhang et al., 2020, 2021a, Tomar et al., 2021] characterize the structural relationships among state dimensions and extract a set of model-invariant state abstractions for RL, while our approach considers the structure among all variables in the system, and besides the invariant part, it also captures the domain-specific factors. Recently, [Zhang et al., 2021b] proposed a method that combines BlockMDPs and a hidden parameter to capture the change across environments.

While the setting is similar, in our representation we not only allow changes in the transition function, but also in observation and reward functions. Moreover, we learn a disentangled representation for the changing parameters that only affect certain components of the state vector.

7 Limitations and future work

In this paper, we proposed AdaRL, a principled framework for transfer RL. AdaRL learns a latent representation with domain-shared and domain-specific components across source domains, uses it to learn an optimal policy parametrized by the domain-specific parameters, and applies it to a new target domain without any further policy optimization, but just by estimating the values of the domain-specific parameters in the target domain. As opposed to previous work, AdaRL can model changes in the state dynamics, observation function and reward function in an unified manner.

We are cautious to claim that the learned representation is the true generative model, since it is not identifiable in general. In future work, we will investigate practical assumptions to allow identification. Currently, our model only uses data from the target to estimate the domain-specific parameters from an arbitrary policy. A future direction is to exploit the target domain to fine-tune the policy.

Finally, we considered policy transfer across domains in the same task. However, it is important to transfer knowledge across different tasks, e.g., different Atari games, which will be our next step. While our work is a first step in a principled framework for policy transfer in RL, our assumptions might not be true in general in real-world applications. The misuse of the method when these assumptions might not hold, could lead to negative impacts, e.g. in safety-critical applications, as self-driving cars.

References

R. Amit and R. Meir. Meta-learning by adjusting priors based on extended pac-bayes theory. In *International Conference on Machine Learning*, pages 205–214, 2018.

C. M. Bishop. Mixture density networks. In *Technical Report NCRG/4288, Aston University, Birmingham, UK*, 1994.

C. Boutilier, R. Dearden, and M. Goldszmidt. Stochastic dynamic programming with factored representations. *Artificial Intelligence*, 121(1-2):49–107, 2000.

G. Brockman, V. Cheung, L. Pettersson, J. Schneider, J. Schulman, J. Tang, and W. Zaremba. Openai gym. *arXiv preprint arXiv:1606.01540*, 2016.

Y. Duan, J. Schulman, X. Chen, P. L. Bartlett, I. Sutskever, and P. Abbeel. Rl²: Fast reinforcement learning via slow reinforcement learning. *arXiv preprint arXiv:1611.02779*, 2016.

L. Espeholt, H. Soyer, R. Munos, K. Simonyan, V. Mnih, T. Ward, Y. Doron, V. Firoiu, T. Harley, I. Dunning, S. Legg, and K. Kavukcuoglu. IMPALA: Scalable distributed deep-rl with importance weighted actor-learner architectures. *ICML*, 2018.

F. Fernández, J. García, and M. Veloso. Probabilistic policy reuse for inter-task transfer learning. *Robotics and Autonomous Systems*, 58(7):866–871, 2010.

C. Finn, P. Abbeel, and S. Levine. Model-agnostic meta-learning for fast adaptation of deep networks. In *International Conference on Machine Learning*, pages 1126–1135, 2017.

S. Gamian and Y. Goldberg. Transfer learning for related reinforcement learning tasks via image-to-image translation. *arXiv preprint arXiv:1806.07377*, 2018.

A. Ghassami, N. Kiyavash, B. Huang, and K. Zhang. Multi-domain causal structure learning in linear systems. *NeurIPS*, 2018.

A. Gupta, B. Eysenbach, C. Finn, and S. Levine. Unsupervised meta-learning for reinforcement learning. *arXiv preprint arXiv:1806.04640*, 2018.

M. Hessel, H. Soyer, L. Espeholt, S. Czarnecki, W. and Schmitt, and H. van Hasselt. Multi-task deep reinforcement learning with popart. *AAAI*, 2019.

T. Hester, M. Vecerik, O. Pietquin, M. Lanctot, T. Schaul, B. Piot, D. Horgan, J. Quan, A. Sendonaris, I. Osband, G. Dulac-Arnold, J. Agapiou, J. Z. Leibo, and A. Gruslys. Deep q-learning from demonstrations. *AAAI*, 2018.

G. E. Hinton and R. R. Salakhutdinov. Reducing the dimensionality of data with neural networks. *Science*, 313(5786):504–507, 2006.

S. Hochreiter and J. Schmidhuber. Long short-term memory. *Neural computation*, 9(8):1735–1780, 1997.

B. Huang*, K. Zhang*, J. Zhang, J. Ramsey, R. Sanchez-Romero, C. Glymour, and B. Schölkopf. Causal discovery from heterogeneous/nonstationary data. *JMLR*, 21(89):612–634, 2020.

M. J. Kearns and D. Koller. Efficient reinforcement learning in factored mdps. *IJCAI*, pages 740–747, 1999. URL <http://ijcai.org/Proceedings/99-2/Papers/013.pdf>.

T. P. Lillicrap, J. J. Hunt, A. Pritzel, N. Heess, T. Erez, Y. Tassa, D. Silver, and D. Wierstra. Continuous control with deep reinforcement learning. *arXiv preprint arXiv:1509.02971*, 2015.

D. A. McAllester. Pac-bayesian model averaging. In *Proceedings of the twelfth annual conference on Computational learning theory*, pages 164–170, 1999.

R. Mendonca, A. Gupta, R. Kralev, P. Abbeel, S. Levine, and C. Finn. Guided meta-policy search. *arXiv preprint arXiv:1904.00956*, 2019.

G. Mesnil, Y. Dauphin, X. Glorot, S. Rifai, Y. Bengio, I. Goodfellow, E. Lavoie, X. Muller, G. Desjardins, D. Warde-Farley, P. Vincent, A. Courville, and J. Bergstra. Unsupervised and transfer learning challenge: a deep learning approach. *JMLR W and CP: Proc. of the Unsupervised and Transfer Learning challenge and workshop*, 27, 2012.

V. Mnih, K. Kavukcuoglu, D. Silver, A. Graves, I. Antonoglou, D. Wierstra, and M. Riedmiller. Playing atari with deep reinforcement learning. *NIPS Deep Learning Workshop*, 2013.

V. Mnih, K. Kavukcuoglu, D. Silver, A. A. Rusu, J. Veness, M. G. Bellemare, A. Graves, M. Riedmiller, A. K. Fidjeland, G. Ostrovski, S. Petersen, C. Beattie, A. Sadik, I. Antonoglou, H. King, D. Kumaran, D. Wierstra, S. Legg, and D. Hassabis. Human-level control through deep reinforcement learning. *Nature*, 518(7540):529–533, 2015.

V. Mnih, A. P. Badia, M. Mirza, A. Graves, T. Lillicrap, T. Harley, P. T. Lillicrap1, D. Silver, and K. Kavukcuoglu. Asynchronous methods for deep reinforcement learning. *ICML*, 2016.

A. Nagabandi, I. Clavera, S. Liu, R. S. Fearing, P. Abbeel, S. Levine, and C. Finn. Learning to adapt in dynamic, real-world environments through meta-reinforcement learning. *arXiv preprint arXiv:1803.11347*, 2018.

A. Y. Ng, D. Harada, and S. Russell. Policy invariance under reward transformations: Theory and application to reward shaping. *ICML*, 1999.

J. Pearl. *Causality: Models, Reasoning, and Inference*. Cambridge University Press, Cambridge, 2000.

A. Pentina and C. Lampert. A pac-bayesian bound for lifelong learning. *ICML*, pages 991–999, 2014.

A. A. Rusu, N. C. Rabinowitz, G. Desjardins, H. Soyer, J. Kirkpatrick, K. Kavukcuoglu, R. Pascanu, and R. Hadsell. Progressive neural networks. *arXiv preprint arXiv:1606.04671*, 2016.

B. Schölkopf. Causality for machine learning. *arXiv preprint arXiv:1911.10500*, 2019.

B. Schölkopf, F. Locatello, S. Bauer, N. R. Ke, N. Kalchbrenner, A. Goyal, and Y. Bengio. Toward causal representation learning. *Proceedings of the IEEE*, 109(5):612–634, 2021a.

B. Schölkopf, F. Locatello, S. Bauer, N. R. Ke, N. Kalchbrenner, A. Goyal, and Y. Bengio. Towards causal representation learning. *CoRR*, abs/2102.11107, 2021b. URL <https://arxiv.org/abs/2102.11107>.

J. Schulman, P. Moritz, S. Levine, M. Jordan, and P. Abbeel. High-dimensional continuous control using generalized advantage estimation. *arXiv preprint arXiv:1506.02438*, 2015.

S. Shalev-Shwartz and S. Ben-David. *Understanding machine learning: From theory to algorithms*. Cambridge university press, 2014.

D. Silver, A. Huang, C. J. Maddison, A. Guez, L. Sifre, G. van den Driessche, J. Schrittwieser, I. Antonoglou, V. Panneershelvam, M. Lanctot, S. Dieleman, D. Grewe, J. Nham, N. Kalchbrenner, I. Sutskever, T. P. Lillicrap, M. Leach, K. Kavukcuoglu, T. Graepel, and D. Hassabis. Mastering the game of go with deep neural networks and tree search. *Nature*, 529:484–489, 2016.

P. Spirtes, C. Glymour, and R. Scheines. *Causation, Prediction, and Search*. Springer-Verlag Lectures in Statistics, 1993.

A. L. Strehl, C. Diuk, and M. L. Littman. Efficient structure learning in factored-state mdps. In *AAAI*, 2007.

R. S. Sutton and A. G. Barto. *Reinforcement Learning: An Introduction*. MIT Press, Cambridge, MA, 1998.

A. Tamar, Y. Glassner, and S. Mannor. Optimizing the cvar via sampling. In *Twenty-Ninth AAAI Conference on Artificial Intelligence*, 2015.

M. E. Taylor and P. Stone. Transfer learning for reinforcement learning domains: A survey. *JMLR*, 10(7), 2009.

M. E. Taylor, P. Stone, and Y. Liu. Transfer learning via inter-task mappings for temporal difference learning. *Journal of Machine Learning Research*, 8(1):2125–2167, 2007.

Y. W. Teh, V. Bapst, W. M. Czarnecki, J. Quan, J. Kirkpatrick, R. Hadsell, N. Heess, and R. Pascanu. DISTRAL: Robust multitask reinforcement learning. *arXiv preprint arXiv:1707.04175*, 2017.

A. Tirinzoni, A. Sessa, M. Pirotta, and M. Restelli. Importance weighted transfer of samples in reinforcement learning. In *International Conference on Machine Learning*, 2018.

A. Tirinzoni, M. Salvini, and M. Restelli. Transfer of samples in policy search via multiple importance sampling. In *International Conference on Machine Learning*, pages 6264–6274, 2019.

M. Tomar, A. Zhang, R. Calandra, M. E. Taylor, and J. Pineau. Model-invariant state abstractions for model-based reinforcement learning, 2021.

H. Van Hasselt, A. Guez, and D. Silver. Deep reinforcement learning with double q-learning. *AAAI*, 2016.

A. Zhang, C. Lyle, S. Sodhani, A. Filos, M. Kwiatkowska, Y. Pineau, J. and Gal, and D. Precup. Invariant causal prediction for block mdps. *arXiv preprint arXiv:2003.06016*, 2020.

A. Zhang, R. McAllister, R. Calandra, Y. Gal, and S. Levine. Learning invariant representations for reinforcement learning without reconstruction. *ICLR*, 2021a.

A. Zhang, S. Sodhani, K. Khetarpal, and J. Pineau. Learning robust state abstractions for hidden-parameter block {mdp}s. In *International Conference on Learning Representations*, 2021b. URL <https://openreview.net/forum?id=fm00I2a3tQP>.

J. Zhang and P. Spirtes. Intervention, determinism, and the causal minimality condition. *Synthese*, 182(3):335–347, 2011.

K. Zhang*, M. Gong*, P. Stojanov, B. Huang, Q. Liu, and C. Glymour. Domain adaptation as a problem of inference on graphical models. *NeurIPS*, 2020.

K. Zhang, J. Peters, D. Janzing, and B. Schölkopf. Kernel-based conditional independence test and application in causal discovery. *arXiv preprint arXiv:1202.3775*, 2020.

Z. Zhu, K. Lin, and J. Zhou. Transfer learning in deep reinforcement learning: A survey. *arXiv preprint arXiv:2009.07888*, 2020.

L. Zintgraf, K. Shiarli, V. Kurin, K. Hofmann, and S. Whiteson. Fast context adaptation via meta-learning. *ICML*, 2019.

A1 Proof of Proposition 1

We first review the definitions of d-separation, the Markov condition, and the faithfulness assumption [Spirtes et al., 1993, Pearl, 2000], which will be used in the proof.

Given a directed acyclic graph $G = (\mathbf{V}, \mathbf{E})$, where \mathbf{V} is the set of nodes and \mathbf{E} is the set of directed edges, we can define a graphical criterion that expresses a set of conditions on the paths.

Definition A1 (d-separation [Pearl, 2000]). *A path p is said to be d-separated by a set of nodes $\mathbf{Z} \subseteq \mathbf{V}$ if and only if (1) p contains a chain $i \rightarrow m \rightarrow j$ or a fork $i \leftarrow m \rightarrow j$ such that the middle node m is in \mathbf{Z} , or (2) p contains a collider $i \rightarrow m \leftarrow j$ such that the middle node m is not in \mathbf{Z} and such that no descendant of m is in \mathbf{Z} .*

Let \mathbf{X} , \mathbf{Y} , and \mathbf{Z} be disjunct sets of nodes. \mathbf{Z} is said to d-separate \mathbf{X} from \mathbf{Y} (denoted as $\mathbf{X} \perp_d \mathbf{Y} | \mathbf{Z}$) if and only if \mathbf{Z} blocks every path from a node in \mathbf{X} to a node in \mathbf{Y} .

Definition A2 (Global Markov Condition [Spirtes et al., 1993, Pearl, 2000]). *A distribution P over \mathbf{V} satisfies the global Markov condition on graph G if for any partition $(\mathbf{X}, \mathbf{Z}, \mathbf{Y})$ such that $\mathbf{X} \perp_d \mathbf{Y} | \mathbf{Z}$*

$$P(\mathbf{X}, \mathbf{Y} | \mathbf{Z}) = P(\mathbf{X} | \mathbf{Z})P(\mathbf{Y} | \mathbf{Z}).$$

In other words, \mathbf{X} is conditionally independent of \mathbf{Y} given \mathbf{Z} , which we denote as $\mathbf{X} \perp \mathbf{Y} | \mathbf{Z}$.

Definition A3 (Faithfulness Assumption [Spirtes et al., 1993, Pearl, 2000]). *There are no independencies between variables that are not entailed by the Markov Condition.*

If we assume both of these assumptions, then we can use d-separation as a criterion to read all of the conditional independences from a given DAG G . In particular, for any disjoint subset of nodes $\mathbf{X}, \mathbf{Y}, \mathbf{Z} \subseteq \mathbf{V}$: $\mathbf{X} \perp \mathbf{Y} | \mathbf{Z} \iff \mathbf{X} \perp_d \mathbf{Y} | \mathbf{Z}$.

We can now prove our main proposition:

Proposition 1. *The minimal domain-generalizable representations contain minimal and sufficient dimensions for policy learning across domains. Moreover, given the graphical representation of the environment model, which is assumed to be Markov and faithful to the measured data, minimal domain-generalizable representations can be identified as:*

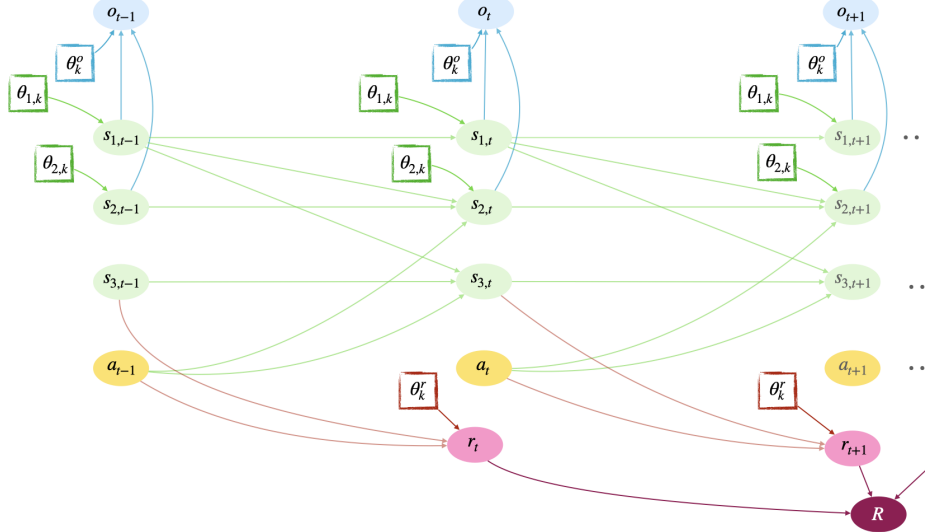
- $\forall s_{i,t} \in \vec{s}_t$, $s_{i,t} \in \vec{s}_t^{sh}$ if and only if there is a direct or indirect edge (i.e. a directed path) from $s_{i,t}$ to $r_{t+\tau}$ (with $\tau \geq 1$).
- $\forall \theta_{i,k} \in \boldsymbol{\theta}_k$, $\theta_{i,k} \in \theta_k^{sp}$ if and only if
 - $\theta_{i,k} \in \theta_k^r$, or
 - $\theta_{i,k} \in \theta_k^s$ and it has a direct or indirect edge to $r_{t+\tau}$ (with $\tau \geq 1$).

Proof. **Part 1:** By definition, in *minimal domain-generalizable representations* every dimension is dependent on a_t given R and any other variables, and every other dimension is independent of a_t given R and some other variables. Furthermore, because every dimension that is dependent on a_t is necessary for the policy learning and every dimension that is (conditionally) independent of a_t for at least a subset of other variables is not necessary for the policy learning, *minimal domain-generalizable representations* contain minimal and sufficient dimensions for policy learning across domains.

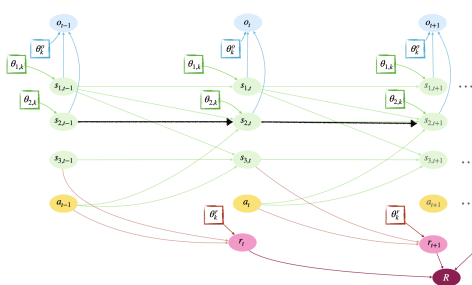
Note that the agents determine the action under the condition of maximizing cumulative reward, which policy learning aims to achieve, so *minimal domain-generalizable representations* always consider the situation when the discounted cumulative reward R is given.

Part 2: Next, we show that with the Markov condition and faithfulness assumption, *minimal domain-generalizable representations* can be directly identified from graphical representations corresponding to the environment model. Moreover, since *minimal domain-generalizable representations* include *minimal domain-shared representations* \vec{s}_t^{sh} and *minimal domain-specific representations* $\boldsymbol{\theta}_k^{sp}$, it is equivalent to show that both \vec{s}_t^{sh} and $\boldsymbol{\theta}_k^{sp}$ can be directly identified from graphical representations corresponding to the environment model.

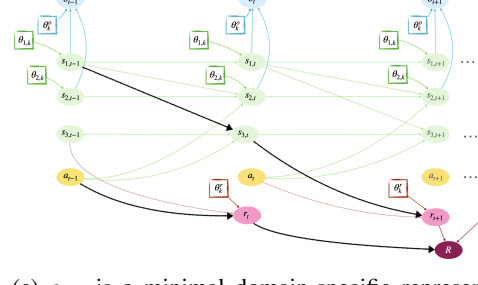
“only if”: We first show that if $s_{i,t} \in \vec{s}_t^{sh}$, then it has a direct or indirect edge to $r_{t+\tau}$, and that if $\theta_{i,k} \in \boldsymbol{\theta}_k^{sp}$, then (1) $\theta_{i,k} \in \theta_k^r$, or (2) $\theta_{i,k} \in \theta_k^s$ and it has a direct or indirect edge to $r_{t+\tau}$ (with $\tau \geq 1$).



(a) The complete example graph without the error terms.



(b) $s_{2,t}$ is not a minimal domain-specific representation, since there is no directed path to any $r_{t+\tau}$, i.e. $s_{2,t} \perp\!\!\!\perp a_t | R$. Similarly, there is no directed path from $\theta_{1,k}$ to R .



(c) $s_{1,t}$ is a minimal domain-specific representation, since there exists a path to a_t that is d-connected when we condition on the collider R . Similarly $\theta_{1,k}$ is d-connected to a_t when conditioning on R .

Figure A1: Example model in which $s_{1,t}$ and $s_{3,t}$ are minimal domain-specific representations for policy learning, while $s_{2,t}$ is not. This does not mean that $s_{2,t}$ and $\theta_{2,k}$ are not useful in the model estimation part, especially in estimating θ_k^o .

We prove it by contradiction. Suppose that $s_{i,t} \in \bar{s}_t^{sh}$ does not have a direct or indirect edge to $r_{t+\tau}$. By assumption a_t only affects \bar{s}_{t+1} , so $s_{i,t} \perp\!\!\!\perp a_t$. Moreover, according to the Markov and faithfulness conditions, $s_{i,t}$ is independent of a_t conditioning on R , since there is no path that connects $s_{i,t} \rightarrow \dots \rightarrow r_{t+\tau} \rightarrow R \leftarrow r_t \leftarrow a_t$ on which R is a collider, which is the only path which could introduce a conditional dependence. Hence, $s_{i,t}$ is not necessary for decision making, and thus $s_{i,t}$ is not a dimension in \bar{s}_t^{sh} , which contradicts the assumption.

Similarly, by contradiction suppose that $\theta_{i,k} \in \theta_k^{sp}$, but it is not a change parameter for the reward function $\theta_{i,k} \notin \theta_k^r$, nor it is a change parameter for the state dynamics $\theta_{i,k} \in \theta_k^s$ without any direct or indirect edge (i.e. a directed path) to $r_{t+\tau}$ for any $\tau \geq 1$. By assumption of our model, $\theta_{i,k}$ is never connected to a_t directly, nor they might have a common cause, so $\theta_{i,k} \perp\!\!\!\perp a_t$. Moreover, according to the Markov condition, $\theta_{i,k}$ is independent of a_t conditioning on R , since:

- if $\theta_{i,k} \notin \theta_k^r$ then it there is no path $\theta_{i,k} \rightarrow s_{i,t+\tau} \rightarrow r_{t+\tau} \rightarrow R \leftarrow r_t \leftarrow a_t$ for any $\tau \in \mathbb{N}$ that would be open by conditioning on R ;

- if $\theta_{i,k} \in \theta_k^s$ but there is no directed path to $r_{t+\tau}$ for any $\tau \geq 1$, i.e. then there is also no directed path $\theta_{i,k} \rightarrow \dots \rightarrow r_{t+\tau} \rightarrow R \leftarrow r_t \leftarrow a_t$ that would be open when we condition on R .

Hence, $\theta_{i,k}$ is not necessary for decision making, and thus $\theta_{i,k}$ is not a dimension in θ_k^{sp} , which contradicts to the assumption.

“if”: We next show that if $s_{i,t}$ has a direct or indirect edge to $r_{t+\tau}$, then $s_{i,t} \in \vec{s}_t^{sh}$, and that if (1) $\theta_{i,k} \in \theta_k^r$, or (2) $\theta_{i,k} \in \theta_k^s$ and it has a direct or indirect edge to $r_{t+\tau}$, then $\theta_{i,k} \in \theta_k^{sp}$.

We prove it by contradiction. Suppose $s_{i,t}$ has a directed path to $r_{t+\tau}$ and it is not a dimension in \vec{s}_t^{sh} . It means that $s_{i,t}$ is independent on a_t given R and a subset of other variables $\vec{s}_t \subseteq \vec{s}_t \setminus s_{i,t}$. Since we assume that there are no instantaneous causal relations across the state dimensions, if $s_{i,t} \not\perp\!\!\!\perp a_t | R$ there can never be an $s_{j,t}$ such that $s_{i,t} \perp\!\!\!\perp a_t | R, s_{j,t}$. In this case, this means that $s_{i,t} \perp\!\!\!\perp a_t | R$ has to hold. Then according to the Markov and faithfulness assumptions, $s_{i,t}$ cannot have any directed path to any $r_{t+\tau} \forall \tau \geq 1$, because that any such path create a v-structure in the collider R , which would be open if we condition on R , contradicting the assumption.

Similarly, suppose $\theta_{i,k}$ is not a dimension in θ_k^{sp} that has a directed path to $r_{t+\tau}$. This means that $\theta_{i,k}$ is independent on a_t given R and some other variables $\tilde{l}_t \subseteq \{\vec{s}_t, \{\theta_k \setminus \theta_{i,k}\}\}$. We distinguish three cases:

- if $\theta_{i,k} \in \theta_k^r$ then it cannot be independent of a_t except by conditioning on r_t , which is not in \tilde{l}_t , so we have a contradiction;
- if $\theta_{i,k} \in \theta_k^s$, then at timestep t it is always only connected to the corresponding $s_{i,t}$. So if there is a directed path π to $r_{t+\tau}$, it has to go through $s_{i,t}$. While π can be blocked by conditioning on $s_{i,t}$, there are infinite past and future paths with the same structure, e.g. through $s_{i,t+1}$ that will not be blocked by conditioning only on variables at timestep t . Under the faithfulness and Markov assumption this means that $\theta_{i,k}$ cannot be independent from a_t by conditioning on any subset of state variables at timestep t or any other change parameters, which is a contradiction.

□

A2 Proof of Theorem 1

In this section, we derive the generalization bound under the PAC-Bayes framework [McAllester, 1999, Shalev-Shwartz and Ben-David, 2014], and our formulation follows [Pentina and Lampert, 2014] and [Amit and Meir, 2018]. We assume that all domains share the sample space \mathcal{Z} , hypothesis space \mathcal{H} , and loss function $\ell : \mathcal{H} \times \mathcal{Z} \rightarrow [0, 1]$. All domains differ in the unknown sample distribution E_k parameterized by θ_k associated with each domain k . We observe the training sets S_1, \dots, S_n corresponding to n different domains. The number of samples in domain k is denoted by m_k . Each dataset S_k is assumed to be generated from an unknown sample distribution $E_k^{m_k}$. We also assume that the sample distribution E_k are generated *i.i.d.* from an unknown domain distribution τ . More specifically, we have $S_k = (z_{k,1}, \dots, z_{k,m}, \dots, z_{k,m_k})$, where $z_{k,m} = (\vec{s}_{k,m}, v^*(\vec{s}_{k,m}))$. Note that, $\vec{s}_{k,m}$ is the m -th state sampled from k -th domain and $v^*(\vec{s}_{k,m})$ is its corresponding optimal value. For any value function $h_\theta(\cdot)$ parameterized by θ , we define the loss function $\ell(h_\theta, z_{k,m}) = D_{dist}(h_\theta(\vec{s}_{k,m}), v^*(\vec{s}_{k,m}))$. We also let P be the prior distribution over \mathcal{H} and Q the posterior over \mathcal{H} .

Theorem 1. *Let \mathcal{Q} be an arbitrary distribution over θ and \mathcal{P} the prior distribution over θ . Then for any $\delta \in (0, 1]$, with probability at least $1 - \delta$, the following inequality holds uniformly for all distributions \mathcal{Q} ,*

$$\begin{aligned} er(\mathcal{Q}) &\leq \frac{1}{n} \sum_{k=1}^n \hat{er}(\mathcal{Q}, S_k) + \frac{1}{n} \sum_{k=1}^n \sqrt{\frac{1}{2(m_k - 1)} \left(D_{KL}(\mathcal{Q} || \mathcal{P}) + \log \frac{2nm_k}{\delta} \right)} \\ &\quad + \sqrt{\frac{1}{2(n-1)} \left(D_{KL}(\mathcal{Q} || \mathcal{P}) + \log \frac{2n}{\delta} \right)}, \end{aligned}$$

where $er(\mathcal{Q})$ and $\hat{er}(\mathcal{Q}, S_k)$ are the generalization error and the training error between the estimated value and the optimal value, respectively.

Proof. This proof consists of two steps, both using the classical PAC-Bayes bound [McAllester, 1999, Shalev-Shwartz and Ben-David, 2014]. Therefore, we start by restating the classical PCA-Bayes bound.

Theorem A1 (Classical PAC-Bayes Bound, General Notations). *Let \mathcal{X} be a sample space, $P(X)$ a distribution over \mathcal{X} , Θ a hypothesis space. Given a loss function $\ell(\theta, X) : \Theta \times \mathcal{X} \rightarrow [0, 1]$ and a collection of M i.i.d random variables (X_1, \dots, X_M) sampled from $P(X)$, let π be a prior distribution over hypothesis in Θ . Then, for any $\delta \in (0, 1]$, the following bound holds uniformly for all posterior distributions ρ over Θ ,*

$$\begin{aligned} P \left(\mathbb{E}_{X_i \sim P(X), \theta \sim \rho} [\ell(\theta, X_i)] \leq \frac{1}{M} \sum_{m=1}^M \mathbb{E}_{\theta \sim \rho} [\ell(\theta, X_m)] + \sqrt{\frac{1}{2(M-1)} \left(D_{KL}(\rho || \pi) + \log \frac{M}{\delta} \right)} \right), \forall \rho \\ \geq 1 - \delta. \end{aligned}$$

Between-domain Generalization Bound First, we bound the between-domain generalization, i.e., relating $er(\mathcal{Q})$ to $er(\mathcal{Q}, E_k)$.

We first expand the generalization error as below,

$$\begin{aligned} er(\mathcal{Q}) &= \mathbb{E}_{(E, m) \sim \tau} \mathbb{E}_{S \sim E^m} \mathbb{E}_{\theta \sim \mathcal{Q}} \mathbb{E}_{h \sim Q(S, \theta)} \mathbb{E}_{z \sim E} \ell(h, z) \\ &= \mathbb{E}_{(E, m) \sim \tau} \mathbb{E}_{S \sim E^m} \mathbb{E}_{\theta \sim \mathcal{Q}} \ell(\theta, E) \\ &= \mathbb{E}_{(E, m) \sim \tau} \mathbb{E}_{S \sim E^m} er(\mathcal{Q}, E). \end{aligned} \quad (\text{A1})$$

Then we compute the error across the training domains,

$$\frac{1}{n} \sum_{k=1}^n \mathbb{E}_{\theta \sim \mathcal{Q}} \mathbb{E}_{h \sim Q(S_k, \theta)} \mathbb{E}_{z \sim E_k} \ell(h, z) = \frac{1}{n} \sum_{k=1}^n er(\mathcal{Q}, E_k). \quad (\text{A2})$$

Then Theorem A1 says that for any $\delta_0 \sim (0, 1]$, we have

$$P \left(er(\mathcal{Q}) \leq \frac{1}{n} \sum_{k=1}^n er(\mathcal{Q}, E_k) + \sqrt{\frac{1}{2(n-1)} \left(D_{KL}(\mathcal{Q} || \mathcal{P}) + \log \frac{n}{\delta_0} \right)} \right) \geq 1 - \delta_0, \quad (\text{A3})$$

where \mathcal{P} is a prior distribution over θ .

Within-domain Generalization Bound Then, we bound the the within-domain generalization, i.e., relating $er(\mathcal{Q}, E_k)$ to $\hat{er}(\mathcal{Q}, S_k)$.

We first have

$$er(\mathcal{Q}, E_k) = \mathbb{E}_{\theta \sim \mathcal{Q}} \mathbb{E}_{h \sim Q(S_k, \theta)} \mathbb{E}_{z \sim E_k} \ell(h, z). \quad (\text{A4})$$

Then we compute the empirical error across the training domains,

$$\hat{er}(\mathcal{Q}, S_k) = \frac{1}{m_k} \sum_{j=1}^{m_k} \mathbb{E}_{h \sim Q(S_k, \theta)} \mathbb{E}_{z \sim E_k} \ell(h, z_{i,j}). \quad (\text{A5})$$

According to Theorem A1, for any $\delta_D \sim (0, 1]$, we have

$$P \left(er(\mathcal{Q}, E_k) \leq \hat{er}(\mathcal{Q}, S_k) + \sqrt{\frac{1}{2(m_k-1)} \left(D_{KL}(\rho || \pi) + \log \frac{m_k}{\delta_k} \right)} \right) \geq 1 - \delta_k. \quad (\text{A6})$$

Since [Amit and Meir, 2018] showed that $D_{KL}(\rho || \pi) \geq D_{KL}(\mathcal{Q} || \mathcal{P})$, the above inequality can be further written as,

$$P \left(er(\mathcal{Q}, E_k) \leq \hat{er}(\mathcal{Q}, S_k) + \sqrt{\frac{1}{2(m_k-1)} \left(D_{KL}(\mathcal{Q} || \mathcal{P}) + \log \frac{m_k}{\delta_k} \right)} \right) \geq 1 - \delta_k. \quad (\text{A7})$$

Overall Generalization Bound Combining Eq. (A3) and (A7) using the union bound and choosing that for any $\delta > 0$, set $\delta_0 \doteq \frac{\delta}{2}$ and $\delta_k \doteq \frac{\delta}{2n}$ for $k = 1, \dots, n$, then we finally obtain,

$$P \left(er(\mathcal{Q}) \leq \frac{1}{n} \sum_{k=1}^n \hat{er}(\mathcal{Q}, S_k) + \frac{1}{n} \sum_{k=1}^n \sqrt{\frac{1}{2(m_k - 1)} \left(D_{KL}(\mathcal{Q} || \mathcal{P}) + \log \frac{2nm_k}{\delta} \right)} \right. \\ \left. + \sqrt{\frac{1}{2(n-1)} \left(D_{KL}(\mathcal{Q} || \mathcal{P}) + \log \frac{2n}{\delta} \right)} \right) \geq 1 - \delta. \quad (\text{A8})$$

□

A3 More details for model estimation

A3.1 Locating model changes

In real-world scenarios, it is often the case that changes to the environment are sparse and localized. Instead of assuming every function to change arbitrarily, which is inefficient and unnecessarily complex, we first identify possible locations of the changes. To this end, we concatenate data from different domains and denote by C the variable that takes distinct values $1, \dots, n$ to represent the domain index. Then, we exploit (conditional) independencies/dependencies to locate model changes. These (conditional) independencies/dependencies can be tested by kernel-based conditional independence tests [Zhang et al., 2020], which allows for both linear or nonlinear relationships between variables. The following proposition considers the identifiability of changing locations in scenarios of both MDP and POMDP.

Proposition A1. *In the scenario of MDP, under the Markov condition and faithfulness assumption, we can uniquely localize the changes by testing conditional independence relationships, no matter what and where the changes are.*

In the scenario of POMDP, we can uniquely localize the changing functions by testing conditional independence relationships, in the following cases:

- if $o_t \perp\!\!\!\perp C$, then there is neither a change in the observation function nor in the state dynamics for any state that is an input to the observation function;
- if $o_t \perp\!\!\!\perp C$ and $a_t \not\perp\!\!\!\perp C | r_{t+1}$, then there is only a change in the reward function;
- if $a_t \perp\!\!\!\perp C | r_{t+1}$, then there is neither a change in the reward function nor in the state dynamics for any state in \bar{s}^{sh} ;
- if $a_t \perp\!\!\!\perp C | r_{t+1}$ and $o_t \not\perp\!\!\!\perp C$, then there is a change in the observation function, or there exists a state that is not in \bar{s}^{sh} but is an input to the observation function, whose dynamics has a change.

Proof. We first formulate the problem as follows. We concatenate data from different domains and use domain-index variable C to indicate whether the corresponding causal mechanism has changes across domains. Specifically, by assuming the Markov condition and faithfulness assumption, $s_{i,t}$ has an edge with C if and only if $p(s_{i,t} | PA(s_{i,t}))$ changes across domains, where $PA(\cdot)$ denotes its parents. Similarly, r_t has an edge with C if and only if $p(r_t | PA(r_t))$ changes across domains, and o_t has an edge with C if and only if $p(o_t | PA(o_t))$ changes across domains. Under this setting, locating changes is equivalent to identify which variables have an edge with C from the data.

Part 1: First, we show that in the scenario of MDP, where the states \bar{s}_t are observed, we can uniquely localize the changes by testing conditional independence relationships.

Based on the Markov condition and faithfulness assumption, $s_{i,t}$ has an edge with C if and only if $p(s_{i,t} | PA(s_{i,t}))$ changes across domains, and r_t has an edge with C if and only if $p(r_t | PA(r_t))$ changes across domains. Thus, we can uniquely localize the changes by testing conditional independence relationships,

Part 2: Next, we consider the scenario of POMDP, where we only observe $\{o_t, r_t, a_t\}$ and the underlying states \bar{s}_t are not observed. Below, we consider each case separately.

Part 2.1: Show that if $o_t \perp\!\!\!\perp C$, then there is neither a change in the observation function nor a change in the state dynamics for any state that is an input to the observation function.

We prove it by contradiction. Suppose that there is a change in the observation function and a change in the state dynamics for any state that is an input to the observation function. That is, o_t has an edge with C , and $s_{i,t}$ that has a direct edge to o_t also connects with C . Based on faithfulness assumption, $o_t \not\perp\!\!\!\perp C$, which contradicts to the assumption. Since we have a contradiction, it must be that there is neither a change in the observation function nor a change in the state dynamics for any state that is an input to the observation function.

Part 2.2: Show that if $o_t \perp\!\!\!\perp C$ and $a_t \not\perp\!\!\!\perp C|r_{t+1}$, then there is only a change in the reward function.

If $o_t \perp\!\!\!\perp C$ and $a_{t-1} \not\perp\!\!\!\perp C|r_t$, based on the Markov condition and faithfulness assumption, r_t has an edge with C , and $s_{i,t}$ and o_t do not have edges with C ; that is, there are only changes in the reward function.

Part 2.3: Show that if $a_t \perp\!\!\!\perp C|r_{t+1}$, then there is neither a change in the reward function nor a change in the state dynamics for any state in \bar{s}^{sh} .

By contradiction, suppose that there is a change in the reward function or there exists a state $s_{j,t} \in \bar{s}^{sh}$ that has a change in its dynamics. That is, r_t has an edge with C or corresponding $s_{j,t}$ has an edge with C . Based on faithfulness assumption, $a_t \not\perp\!\!\!\perp C|r_{t+1}$, which contradicts to the assumption.

Part 2.4: Show that if $a_t \perp\!\!\!\perp C|r_{t+1}$ and $o_t \not\perp\!\!\!\perp C$, then there is a change in the observation function, or there exists a state that is not in \bar{s}^{sh} but is an input to the observation function, whose dynamics has a change.

According to Part 2.3, if $a_t \perp\!\!\!\perp C|r_{t+1}$, then there is neither a change in the reward function nor a change in the state dynamics for any state in \bar{s}^{sh} . Furthermore, since $o_t \not\perp\!\!\!\perp C$, then based on the Markov condition, either o_t has an edge with C , or there exists a state that is not in \bar{s}^{sh} but is an input to the observation function, whose dynamics has an edge with C . That is, there is a change in the observation function, or there exists a state that is not in \bar{s}^{sh} but is an input to the observation function, whose dynamics has a change.

□

Based on the above proposition, in the scenario of MDP, we can fully decide what and where the changes are, and we only consider the corresponding $\theta_k^{(\cdot)}$ to capture the changes. In the scenario of POMDP, if there is no change in the observation function (case 1), then in model estimation, we only need to involve θ_k^s and θ_k^r , that is $\theta_k = \{\theta_k^s, \theta_k^r\}$. Similarly, if there are only changes in the reward function (case 2), then we only need to consider θ_k^r , and if there is no change in the reward function (case 3), then $\theta_k = \{\theta_k^o, \theta_k^s\}$, and for case 4, $\theta_k = \{\theta_k^o, \theta_k^s, \theta_k^r\}$. For other cases, we will involve $\theta_k = \{\theta_k^o, \theta_k^s, \theta_k^r\}$ in model estimation.

A3.2 More details for estimation of domain-varying models in one step

We use MiSS-VAE to learn the environment model, which contains three components: the "sequential VAE" component, the "multi-model" component, and the "structure" component. Figure A2 gives the diagram of neural network architecture in model training.

Specifically, for the "sequential VAE" component, we include a Long Short-Term Memory (LSTM [Hochreiter and Schmidhuber, 1997]) to encode the sequential information with output h_t and a Mixture Density Network (MDN [Bishop, 1994]) to output the parameters of MoGs, and thus to learn the inference model $q_\phi(\vec{s}_{t,k}|\vec{s}_{t-1,k}, \mathbf{y}_{1:t,k}, a_{1:t-1,k}; \theta_k)$ and infer a sample of $\vec{s}_{t,k}$ from q_ϕ as the output. The generated sample further acts as an input to the decoder, and the decoder outputs \hat{o}_{t+1} and \hat{r}_{t+2} . Moreover, the state dynamics which satisfies a Markov process is modeled with an MLP and MDN.

For the "multi-model" component, we include the domain index k as an input to LSTM and involve θ_k as free parameters in the inference model q_ϕ , by assuming that θ_k also characterizes the changes in the inference model. Moreover, we embed θ_k^s in state dynamics p_γ , θ_k^o in observation function and θ_k^r in reward function in the decoder. With such a characterization, except θ_k , all other parameters are shared across domains, so that all we need to update in the target domain is the low-dimensional θ_k ,

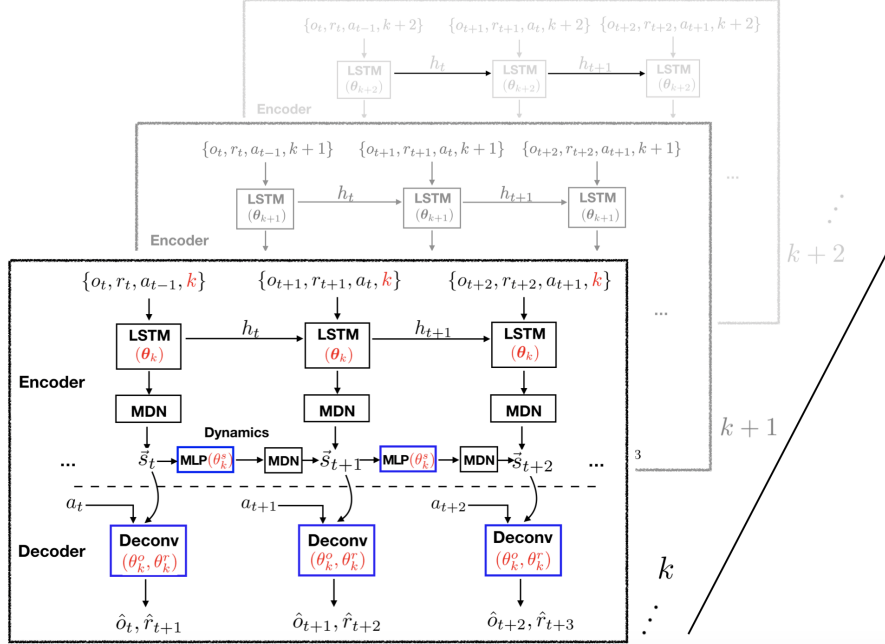


Figure A2: Diagram of MiSS-VAE neural network architecture. The "sequential VAE" component, "multi-model" component, and "structure" component are marked with black, red, and blue, respectively.

which greatly improves the sample efficiency and the statistical efficiency in the target domain—usually few samples are needed.

For the "structure" component, the latent states are organized with structures, captured by structural matrix D . Also, the structural relationships among perceived signals, latent states, the action variable, the reward variable, and the domain-specific factors are embedded as free parameters (structural matrices A, B, C, E, F) into MiSS-VAE.

A4 Complete experimental results

In this section we provide the complete experimental results on both of our settings, modified Cartpole and modified Pong in the OpenAI Gym [Brockman et al., 2016]. We use images as input, which for Cartpole look like Fig. A5(a) and for Pong look like Fig. A10(a).

We consider both changes in the state dynamics (e.g., the change of gravity or cart mass in Cartpole, or the change of orientation in Atari), and changes in perceived signals (e.g., different noise levels on observed images in Cartpole, as shown in Fig. A5, or both noise levels and different colors in Atari, as shown in Fig. A10).

A4.1 Complete results of modified Cartpole experiment

The Cartpole problem consists of a cart and a vertical pendulum attached to the cart using a passive pivot joint. The cart can move left or right. The task is to prevent the vertical pendulum from falling by putting a force on the cart to move it left or right. The action space consists of two actions: moving left or right.

We introduce two changing factors for the state dynamics θ_k^s : varying gravity and varying mass of the cart, and a changing factor in the observation function θ_k^o that is the image noise level. Fig. A3 gives a visual example of Cartpole game, and the image with Gaussian noise. The images of the varying gravity and mass look exactly like the original image.

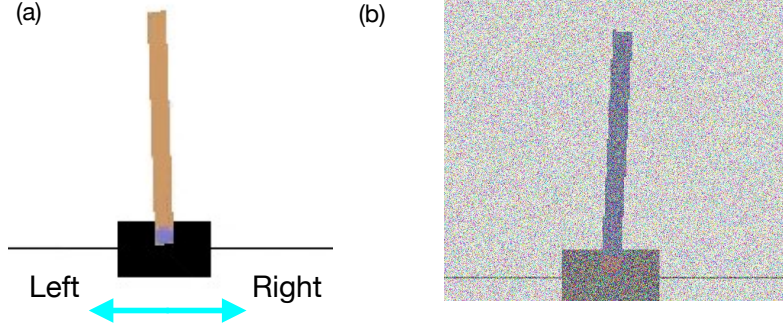


Figure A3: Visual examples of Cartpole game and changing factors. (a) Cartpole game; (b) Modified Cartpole game with Gaussian noise on the image. The light blue arrows are added to show the direction in which the agent can move.

We summarize the detailed settings in both source and target domains in Table A1. In particular in each experiment we use all source domains for each changing factor and one of the target domains at a time in either the interpolation and extrapolation set.

	Gravity	Mass	Noise
Source domains	$\{5, 10, 20, 30, 40\}$	$\{0.5, 1.5, 2.5, 3.5, 4.5\}$	$\{0.25, 0.75, 1.25, 1.75, 2.25\}$
Interpolation set	$\{15, 25, 35\}$	$\{1.0, 2.0, 3.0, 4.0\}$	$\{0.5, 1.0, 1.5, 2.0\}$
Extrapolation set	$\{2, 45, 50, 55\}$	$\{0.2, 5.0, 5.5\}$	$\{0, 2.5, 2.75\}$

Table A1: The settings of source and target domains for modified Cartpole experiments.

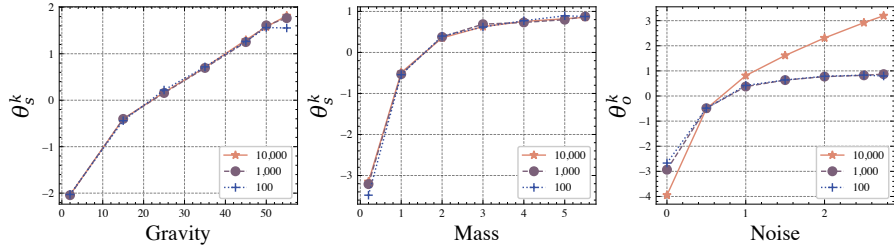


Figure A4: Learned θ_k for changing factors in target domains with different N_{target} .

A4.1.1 Learned θ_k in Cartpole experiments

Fig. A4 shows the estimated θ_k in the modified Cartpole experiments with different N_{target} in the target domains. For the gravity and mass scenarios, the learned parameters with different sample sizes are close with each other. This phenomenon indicates that even with only a few samples (e.g., 100), AdaRL can estimate these change parameters very well. For the noise level factor, the learned curves with different sample sizes have a similar behaviour, but the distance is larger.

In both the noise level and gravity case with $N_{target} = 10,000$, we can see that the θ_k we learn is approximately a linear function of the actual perturbation in gravity and noise, while for the mass it is a monotonic function.

A4.1.2 Average final scores for multiple N_{target} in Cartpole experiments

Fig. A5 shows the complete results of modified Cartpole experiments for $N_{target} = 10,000$, while Fig. A6 provides the same results for different N_{target} .

We average the scores across 30 trials from different random seeds during policy learning stage. We find that the difference between AdaRL and PNN/MAML is larger when N_{target} is small. This

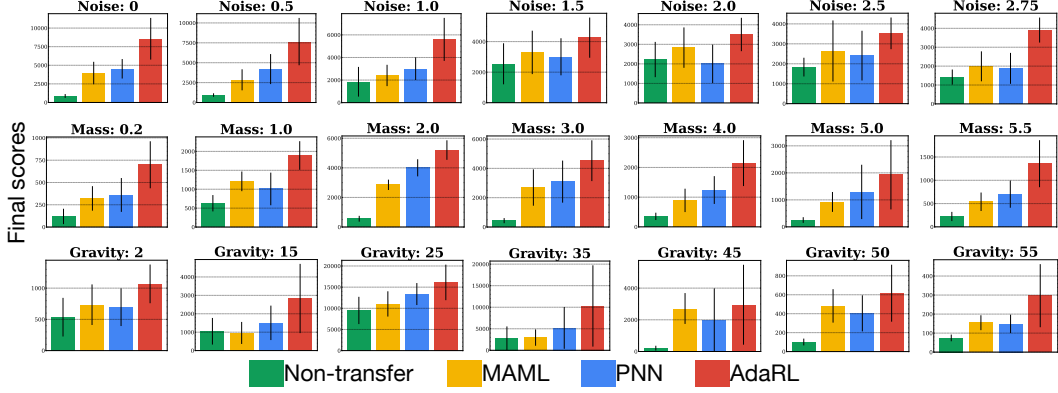


Figure A5: Average final scores on Cartpole across 30 trials with changing gravity, mass, and noise level on input images. Here, $N_{target} = 10,000$, for different values of N_{target} see Fig. A6.

provides some evidence to our conclusion that AdaRL can learn better with fewer samples. Moreover, while PNN and MAML perform as bad as the naive baseline on $N_{target} = 50$ or less, for AdaRL there is a significant improvement from $N_{target} = 5$ to $N_{target} = 10$ samples in the test domain. In some cases, the performances with 10 samples are comparable with those with 10,000 samples.

A4.1.3 Average policy learning curves in terms of steps

Fig. A7, A8, and A9 provide the learning curves for modified Cartpole experiments with multiple changing factors.

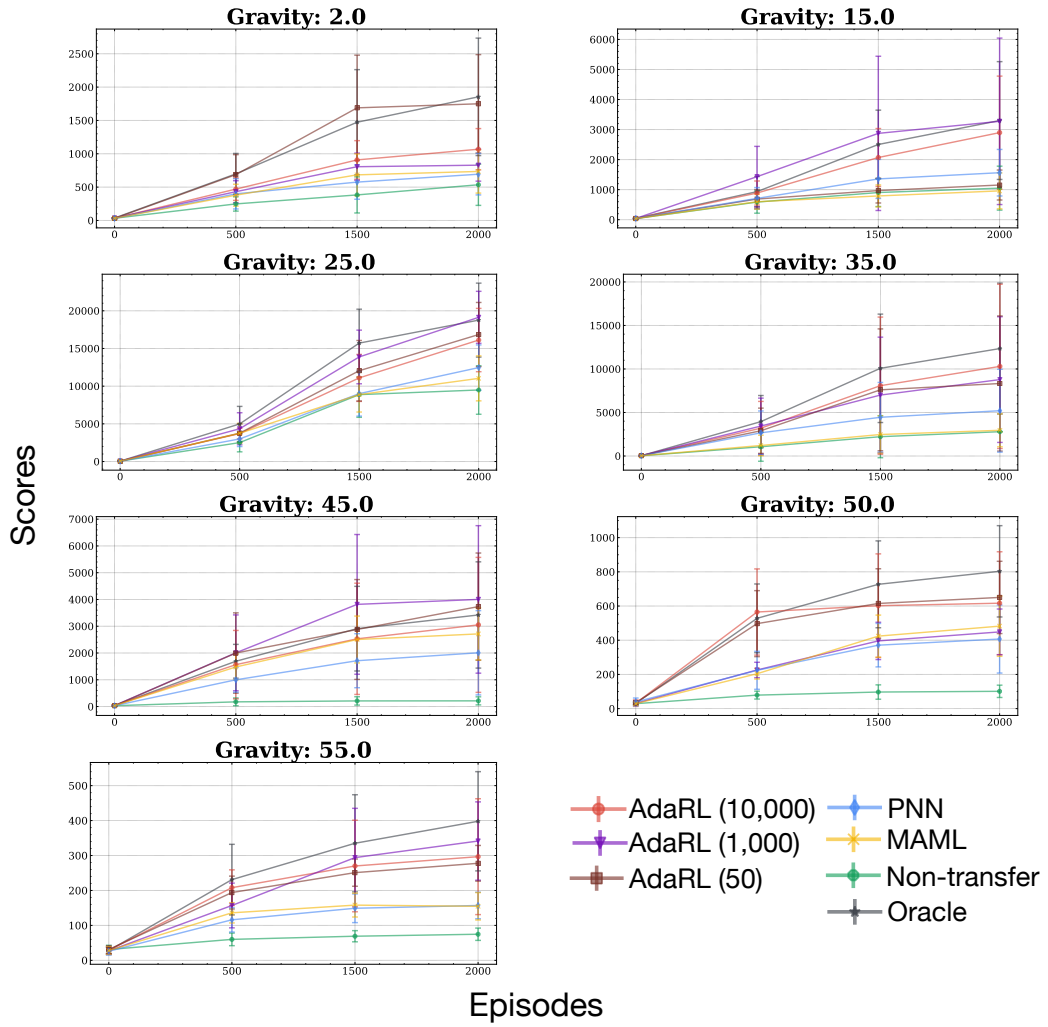


Figure A7: Learning curves for modified Cartpole experiments with changing gravity. The reported scores are averaged across 60 runs. The bars indicate the standard deviation across 60 runs.

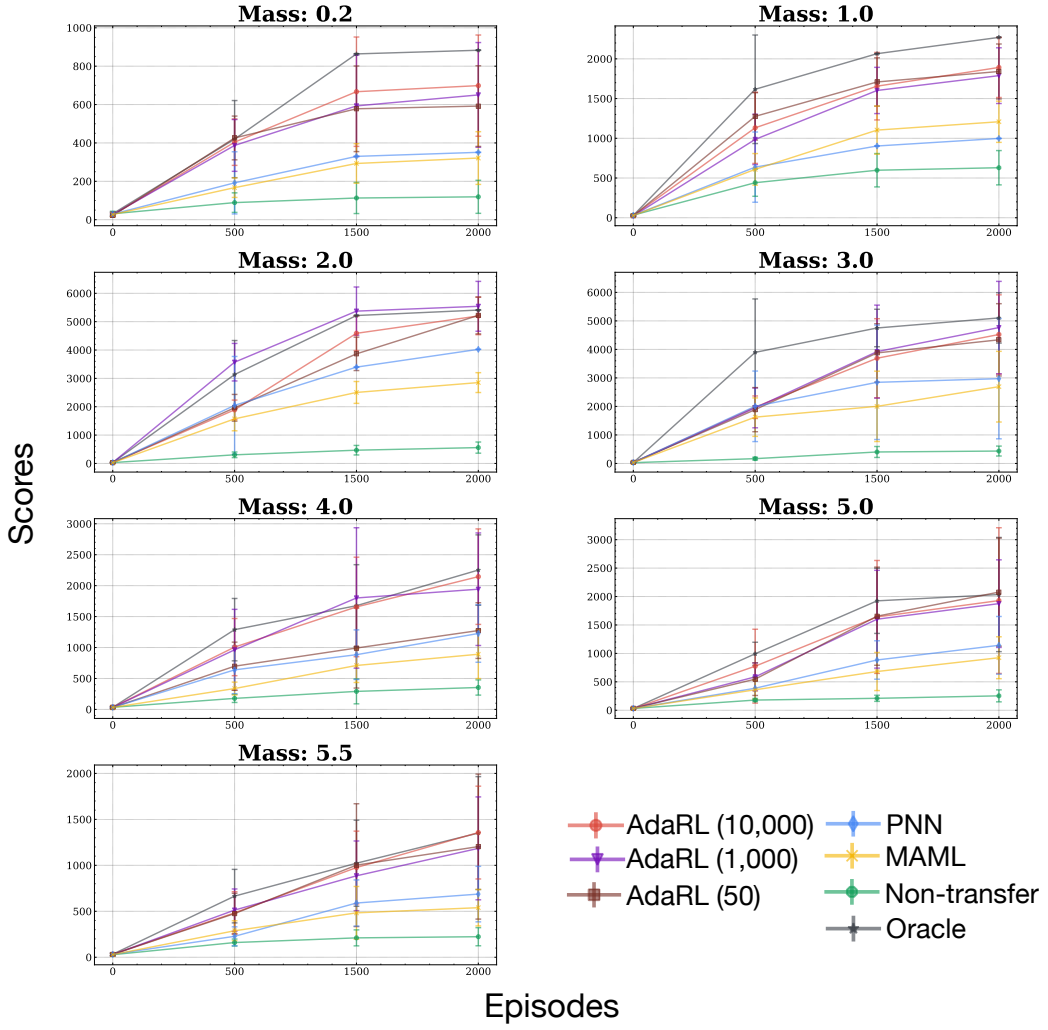


Figure A8: Learning curves for modified Cartpole experiments with changing mass. The reported scores are averaged across 60 runs. The bars indicate the standard deviation across 60 runs.

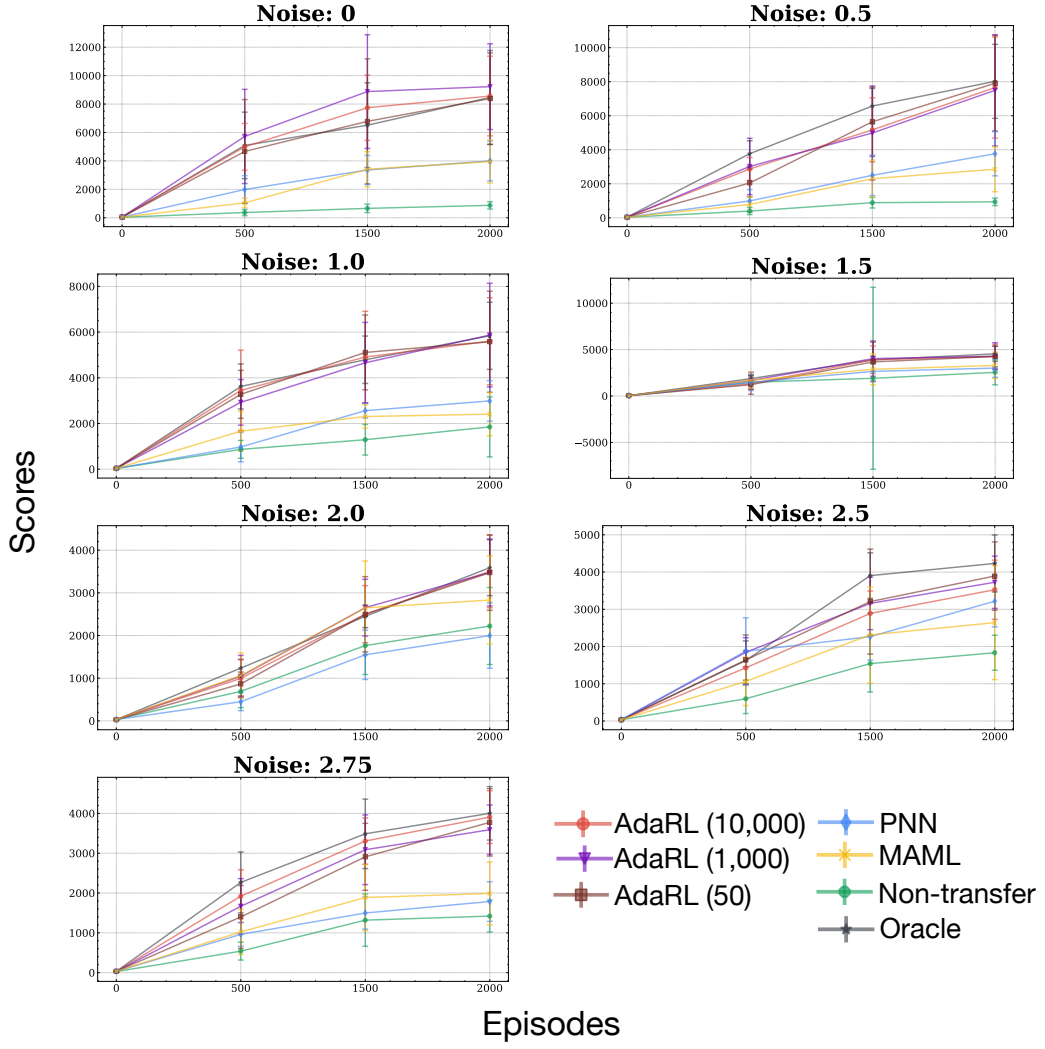


Figure A9: Learning curves for modified Cartpole experiments with changing noise levels. The reported scores are averaged across 60 runs. The bars indicate the standard deviation across 60 runs.

A4.2 Complete results of the modified Pong experiment with changing dynamics and observations

Atari Pong is a two-dimensional game that simulates table tennis. The agent controls a paddle moving up and down vertically, aiming at hitting the ball. The goal for the agent is to reach higher scores, which are earned when the other agent (hard-coded) fails to hit back the ball. We show the example of the original visual inputs and how it appears after we have changed each of the changing factors in Fig. A10.

We summarize the detailed settings in both source and target domains in Table A2. In particular, in each experiment we use all source domains for each changing factor and one of the target domains at a time in either the interpolation and extrapolation set.

	Size	Orientations	Noise	Background colors
Source domains	$\{2, 4, 6, 8\}$	$0^\circ, 180^\circ$	$\{0.25, 0.75, 1.25, 1.75, 2.25\}$	original, green, red
Interpolation set	$\{3, 5, 7\}$	90°	$\{0.5, 1.0, 1.5, 2.0\}$	yellow
Extrapolation set	$\{1, 9\}$	270°	$\{0, 2.75\}$	white

Table A2: The settings of source and target domains for modified Pong experiments.

A4.2.1 Learned θ_k in modified Pong experiments

Fig. A11a, Table A3, and Table A4 show the learned θ_k in modified Pong experiments across different changing factors.

N_{target}	Orientations	0°	90°	180°	270°
10,000	θ_k^{s1}	-2.39	-1.65	1.93	0.58
	θ_k^{s2}	-3.17	-2.01	1.86	1.40
1,000	θ_k^{s1}	-1.98	-1.49	1.73	0.67
	θ_k^{s2}	-2.64	-1.97	1.21	1.13
50	θ_k^{s1}	-2.01	-0.87	1.85	0.69
	θ_k^{s2}	-2.59	-1.84	1.42	1.07

Table A3: The learned θ_k^s across different orientation angles with different N_{target} . The bold columns represent the target domains.

We can find that each dimension of the learned θ_k^s is a nonlinear monotonic function of the changing factors. Table A3, Table A4 and Fig. A11b also give the learned θ_k^o with different sample sizes N_{target} in target domains. Similarly, the learned curves with different sample sizes are homologous. Even with a few samples, AdaRL can still capture the model changes well.

N_{target}	Colors	Original	Red	Green	Yellow	White
10,000	θ_k^{o1}	1.36	1.47	1.04	1.58	-0.91
	θ_k^{o2}	0.72	-1.15	1.17	0.96	-1.33
	θ_k^{o3}	0.93	-1.28	-1.31	-0.65	-1.09
1,000	θ_k^{o1}	1.25	1.40	0.98	1.31	-0.49
	θ_k^{o2}	0.53	-0.89	0.67	1.07	-0.86
	θ_k^{o3}	0.76	-0.94	-1.07	0.03	-0.97
50	θ_k^{o1}	0.96	1.13	0.82	1.26	-0.73
	θ_k^{o2}	0.59	-0.46	0.75	1.32	-0.59
	θ_k^{o3}	0.61	-1.02	-0.91	-0.18	-0.49

Table A4: The learned θ_k^o across different colors with different N_{target} . The bold columns represent the target domains.

Fig. A12 provides the complete results of the modified Pong experiments. The details of both source and target domains are listed in Table A2. Similar to the results of Cartpole, AdaRL can perform the best among all baselines in Pong experiments.

A4.2.2 Average final scores for multiple N_{target}

Fig. A13 gives the average final scores for multiple N_{target} in modified Pong experiments. As shown in the results of the main paper, AdaRL consistently outperforms the other methods.

A4.2.3 Average policy learning curves in terms of steps

Fig. A14 gives the learning curves for modified Pong experiments with multiple changing factors.

A4.3 Complete results of the modified Pong experiment with changing reward functions

Table A5 summarizes the detailed changing factors in both linear and non-linear reward groups.

	Linear reward (k_1)	Non-linear reward (k_2)
Source domains	{0.1, 0.2, 0.3, 0.4, 0.6, 0.7, 0.8}	{2.0, 3.0, 5.0, 6.0, 7.0, 8.0, 9.0}
Interpolation set	{0.5}	{4.0}
Extrapolation set	{0.9}	{1.0}

Table A5: The settings of source and target domains for modified Pong experiments.

A4.3.1 Learned θ_r in modified Pong experiments

Fig. A15 and A16 give the learned θ_r with both linear and non-linear rewards. In both groups, the learned θ_r is linearly or monotonically correlated with the changing factor k_1 and there is no significant gap between the learned θ_r with different N_{target} .

A4.3.2 Average final scores for multiple N_{target}

Fig. A17 shows the average final scores for multiple N_{target} in modified Pong experiments with changing rewards. AdaRL consistently outperforms the other methods across different N_{target} .

A4.3.3 Average policy learning curves in terms of steps

Fig. A18 gives the learning curves for modified Pong experiments with changing rewards.

A5 Experimental details

Model estimation We use a random policy to collect sequence data from source domains. For both modified Cartpole and Pong experiments, the sequence length is 40 and the number of sequence is 10,000 for each domain. The sampling resolution is set to be 0.02. Other details are summarized in Table A6.

Settings	Cartpole	Pong
# Dimensions of latent space	20	25
# Dimensions of θ	1	Size & noise: 1, orientation: 2, color: 3, Reward: 1 (linear), 2 (non-linear)
# Epochs	1,000	reward-varying: 4,000, others: 1,500
Batch size	20	80
# RNN cells	256	256
Initial learning rate	0.01	0.01
Learning rate decay rate	0.999	0.999
Dropout	0.90	0.90
KL-tolerance	0.50	0.50

Table A6: Experimental details on the model estimation part.

Policy learning We adopt Double DQN [Van Hasselt et al., 2016] during policy learning stage. The detailed hyper-parameters are summarized in Table A7. For a fair comparison, we use the same set of hyperparameters for training the Non-transfer PNN, and MAML.

Settings	Cartpole	Pong
Discount factor	0.99	0.99
Exploration rate	1.0	1.0
Initial learning rate	0.01	0.01
Learning rate decay rate	0.999	0.999
Dropout	0.90	0.90
Update target frequency	10,000	10,000

Table A7: Experimental details on the policy learning part.

A5.1 Experimental platforms

For the model estimation, Cartpole and Pong experiments are implemented on 1 NVIDIA P100 GPUs and 4 NVidia V100 GPUs, respectively. The policy learning stages in both experiments are implemented on 8 Nvidia RTX 1080Ti GPUs.

A5.2 Licenses

In our code, we have used the following libraries which are covered by the corresponding licenses:

- Tensorflow (Apache License 2.0),
- Pytorch (BSD 3-Clause "New" or "Revised" License),
- OpenAI Gym (MIT License),
- OpenCV (Apache 2 License),
- Numpy (BSD 3-Clause "New" or "Revised" License)
- Keras (Apache License).

We plan to release our code under the MIT License.

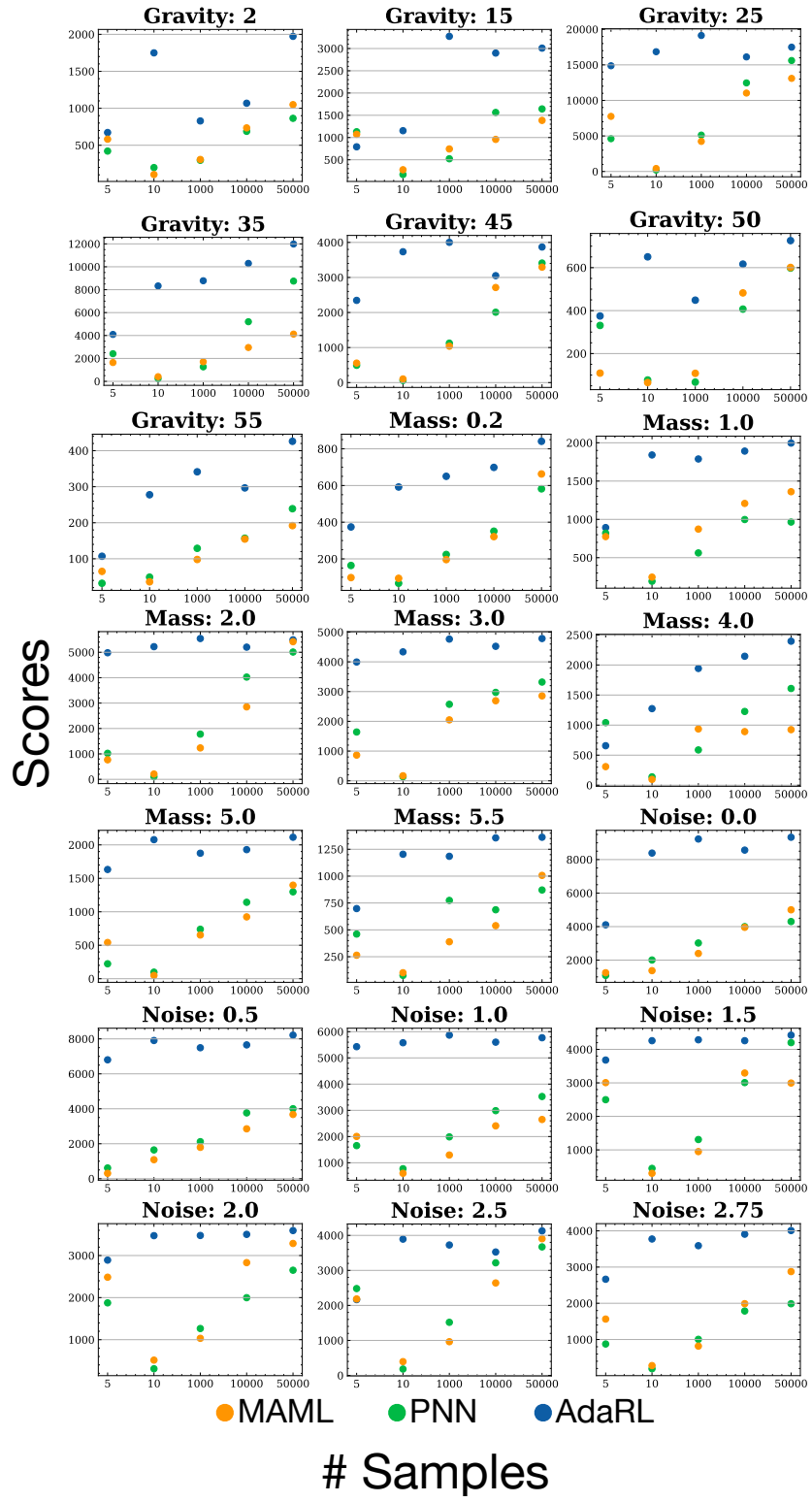


Figure A6: Average final scores on Modified Cartpole experiments with $N_{target} = 5, 10, 1000, 10,000$ and $50,000$.

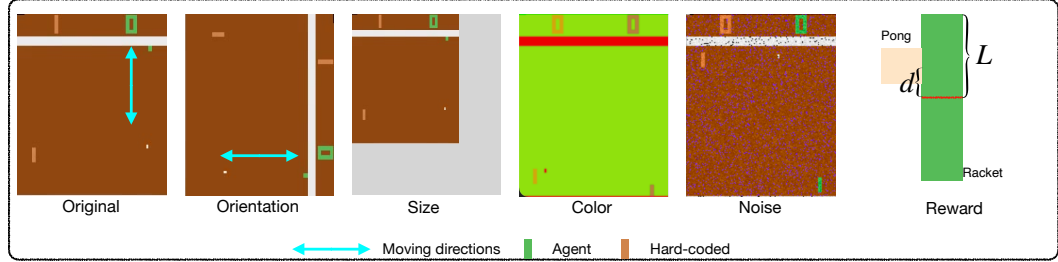


Figure A10: Visual example of the original Pong game and the various changing factors. The light blue arrows are added to show the direction in which the agent can move.

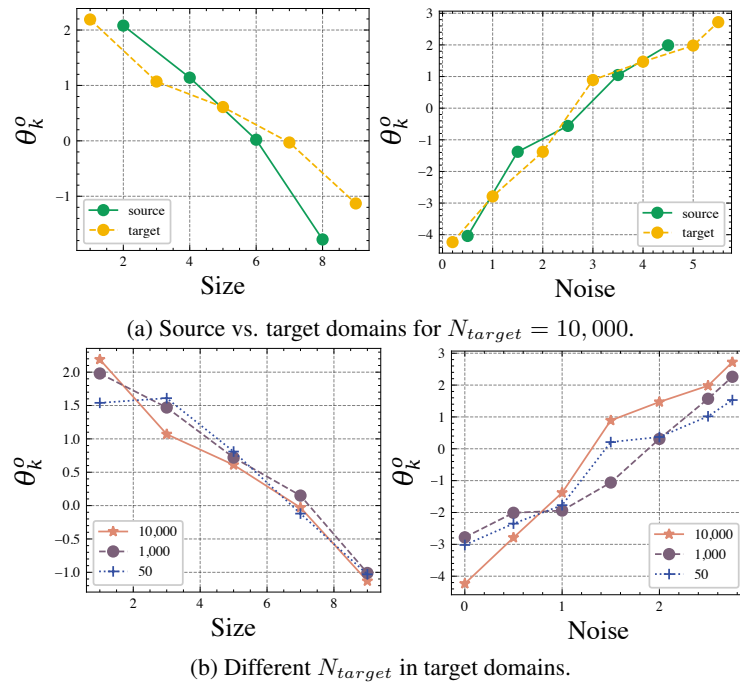


Figure A11: Learned θ_k^o for the two changing factors, size and noise.

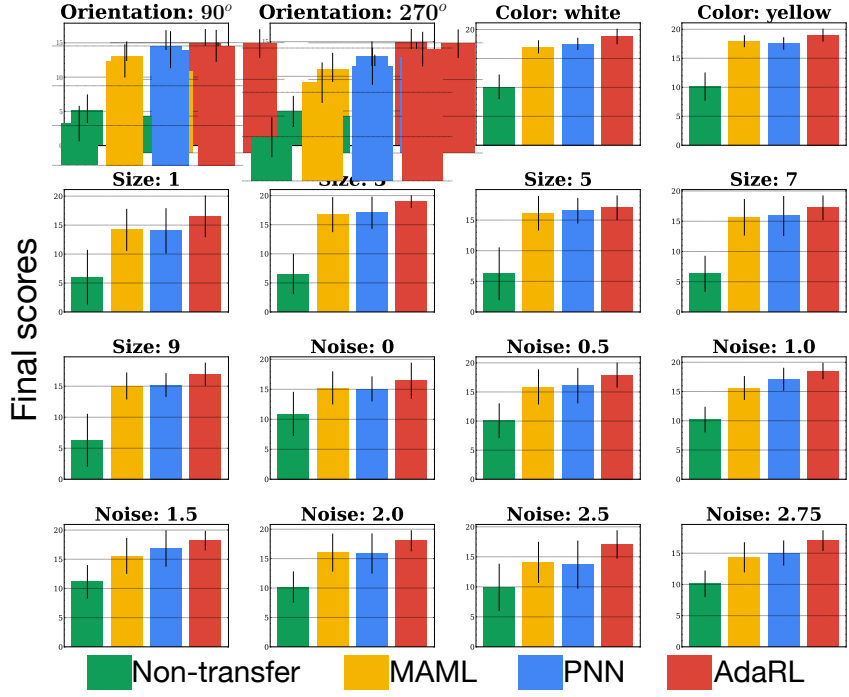


Figure A12: Average final score on Modified Pong across 30 trials with changing orientation, size, color, and noise levels. Here, $N_{target} = 10,000$.

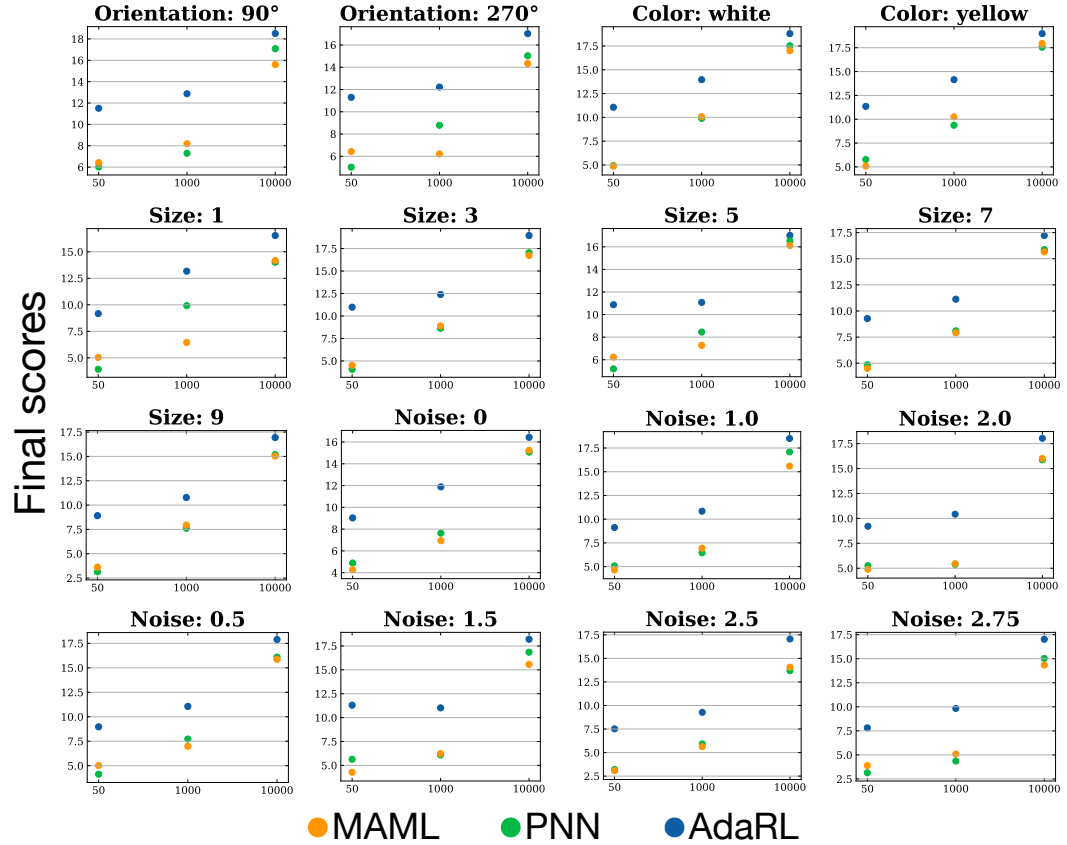


Figure A13: Average final scores on modified Pong across 30 trials with different N_{target} .

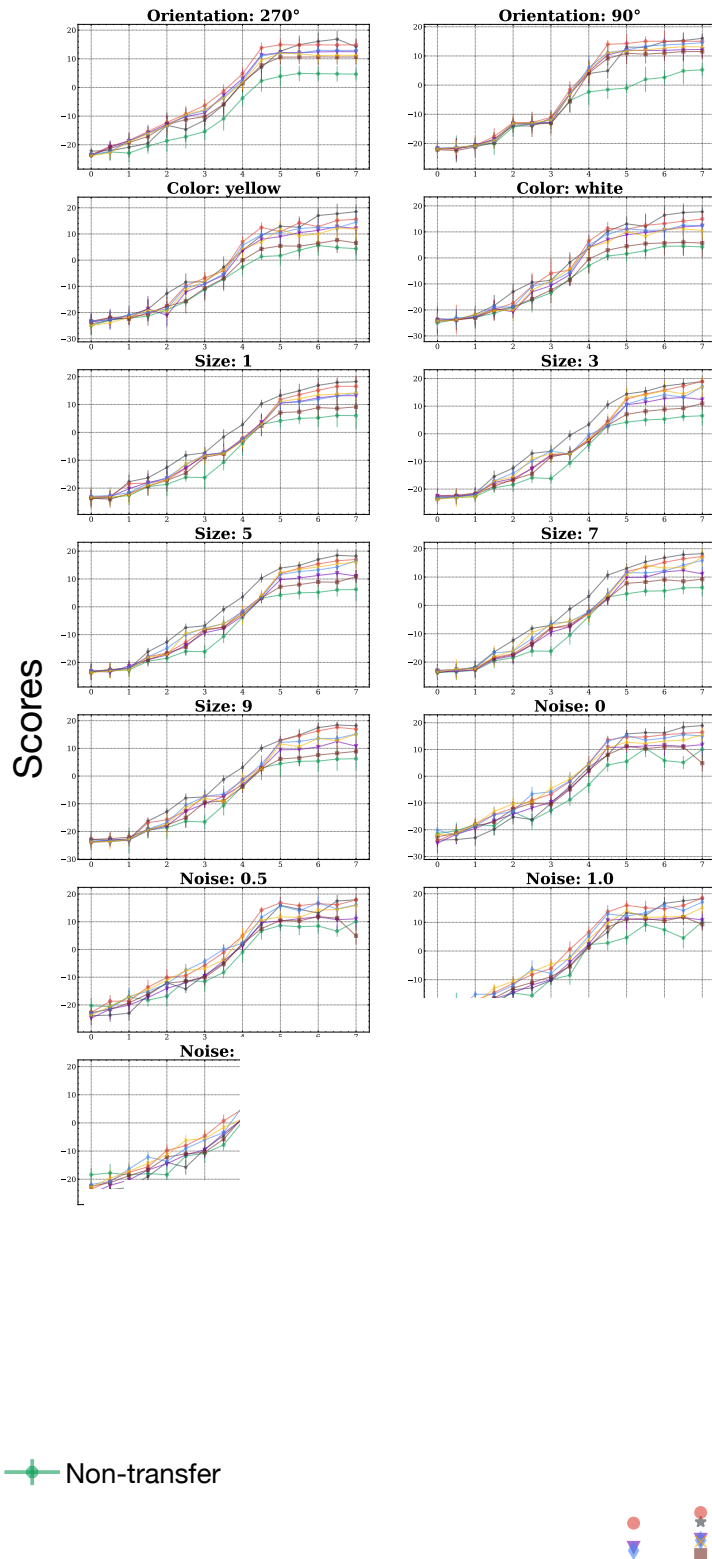
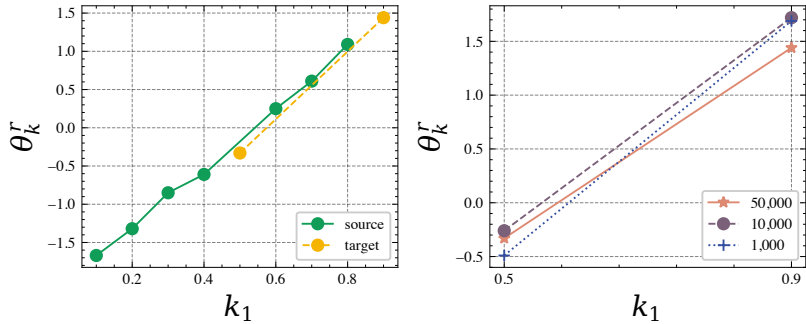
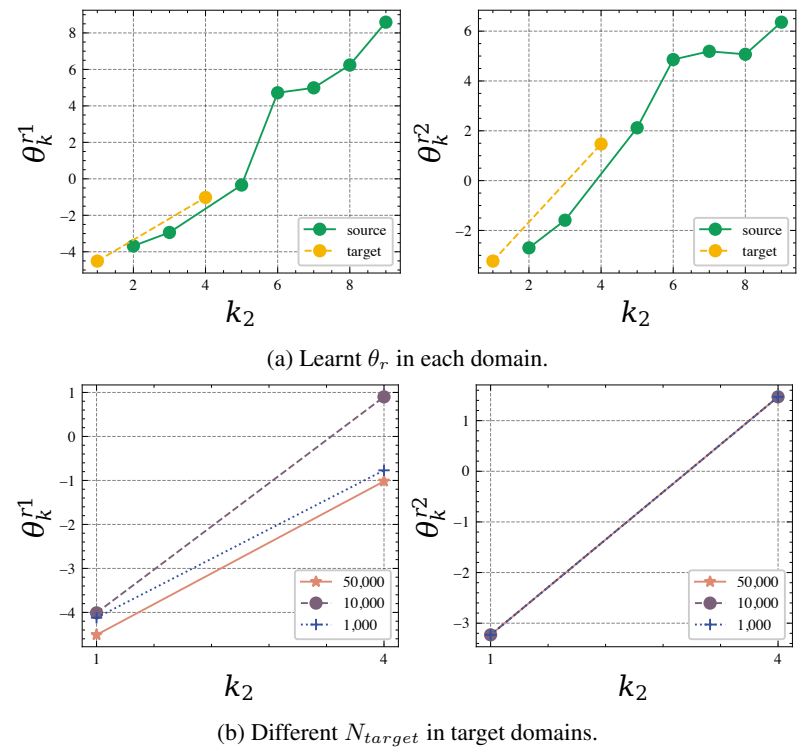


Figure A14: Learning curves for modified Pong. The reported scores are averaged across 30 runs.



(a) Learnt θ_r in each domain. (b) Different N_{target} in target domains.

Figure A15: Learned θ_k^r for the linear changing rewards.



(a) Learnt θ_r in each domain.

(b) Different N_{target} in target domains.

Figure A16: Learned θ_k^r for the non-linear changing rewards.

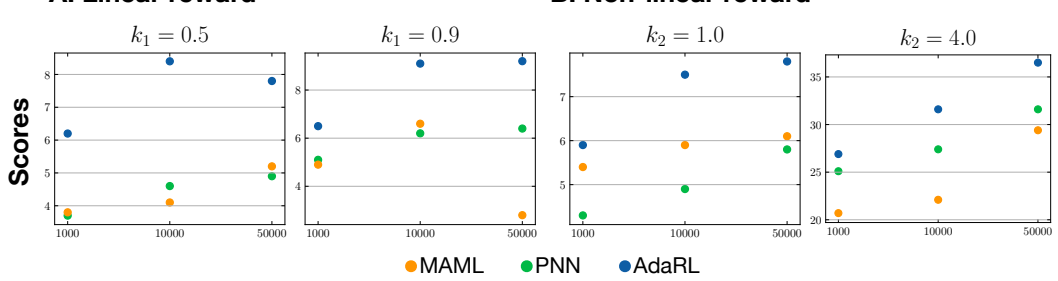


Figure A17: Average final scores on reward-varying Pong experiments across 30 trials with different N_{target} .

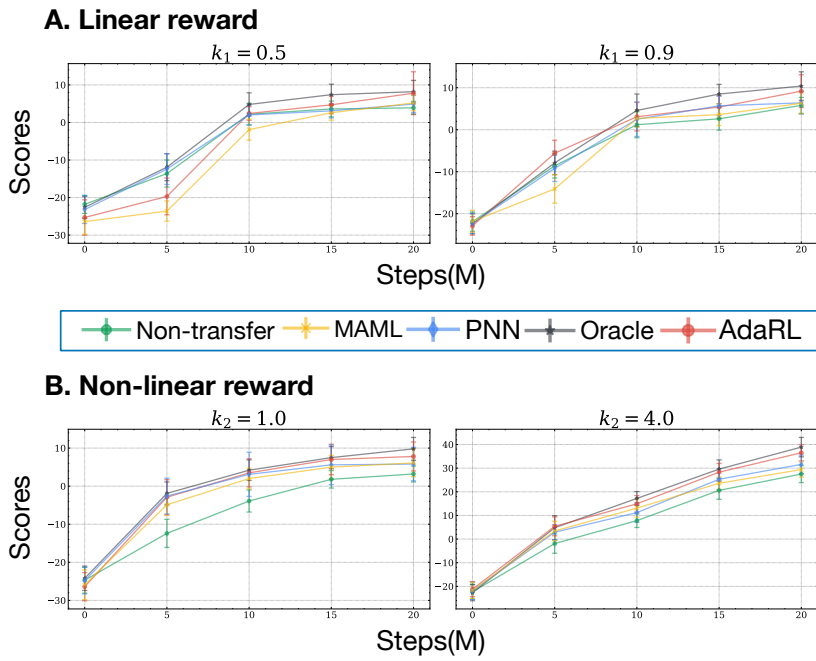


Figure A18: Learning curves for modified Pong experiments with changing reward functions. The reported scores are averaged across 30 runs. The bars indicate the standard deviation across 60 runs.